

# Effects of Melting on Faulting and Continental Deformation

CLAUDIO L. ROSENBERG, SERGEI MEDVEDEV,  
and MARK R. HANDY

Department of Earth Sciences, Freie Universität Berlin, Malteserstr. 74–100,  
12249 Berlin, Germany

## ABSTRACT

The presence of melt is closely related to the localization of deformation in faults and shear zones in a variety of tectonic settings. This relationship is observed on length scales from the outcrop to plate boundary faults to orogens. However, the question of whether melting induces localization, or localization creates a pathway for melts, can rarely be answered from field observations alone. Experimental studies show that rock strength decreases exponentially with increasing volume percentage of melt. This suggests that melting facilitates strain localization where deformation would be homogeneous in the absence of melt. Yet, the extrapolation of experimental relationships between rock strength and melt content to natural conditions at depth in the lithosphere remains speculative, largely because the grain-scale processes underlying dramatic weakening at small amounts of melt have yet to be investigated in crustal rocks. New geochronological methods for dating minerals that crystallized during deformation in the presence of melt have the potential to constrain the time lag between the onset of melting and deformation in naturally deformed anatectic rocks. An indirect, but clear answer to the question of whether melting induces strain localization on a regional scale comes from numerical models of orogenesis which can be run in the presence or absence of low-viscosity domains that approximate the mechanical behavior of partially melted rock. These models show that melting induces lateral flow of anatectic crust within horizontal channels usually situated at the base of the continental crust. These channels have strong vertical strain gradients, especially at their boundaries where shear zones accommodate lateral extrusion of the anatectic rock in between. Together with their bounding shear zones, these flow channels form a new class of faults, which we term “extrusional faults.” Extrusional faults containing long-lived melt (tens of millions of years) can support large, broadly distributed topographic loads

such as orogenic plateaus and can exhume deeply buried rocks from beneath orogens. In contrast, strike-slip and oblique-slip faults serve as steep conduits for the rapid ascent, differentiation, and crystallization of melt. The relatively short residence time of melts in such moderately to steeply dipping fault systems can lead to episodic motion, with long periods of creep punctuated by shorter periods of melt veining, magmatic activity, and/or faster slip.

## INTRODUCTION

Mechanical coupling within the continental lithosphere is manifested by a wide variety of the first-order structural features, from the geometry of faults and shear zones to the topography of orogens (e.g., Royden 1996) and the architecture of passive margins (e.g., Hopper and Buck 1998; Brun 1999). In the absence of melt, the solid-state creep of minerals governs rock rheology and determines the location of decoupling horizons within lithologically and rheologically stratified lithosphere (Ranalli and Murphy 1987). Melting obviously changes rheology and mechanical coupling for the simple reason that melts have very low viscosities compared to that of rock undergoing solid-state creep (Cruden 1990).

This chapter focuses on how melting affects the structure and the rheology of continental crust. As used below, “melting” refers to the process of partial fusion (anatexis) within crust that is subjected to prolonged temperatures above its solidus. Thus, we consider the effects of regional melting on faulting and shearing in the intermediate and lower crust, rather than any local effects associated with flash-heating and ephemeral melting during coseismic slip on fault surfaces in the upper crust (Chapter 5). We note that regional melting usually occurs well below the depth interval of the brittle-to-ductile transition in melt-free crust (Chapter 1), although we hasten to add that melting can certainly induce fracturing during viscous creep, as previously documented in several studies (e.g., Handy et al. 2001, and references therein).

The dramatic weakening effect of melt in crustal rocks has been known for several decades, both from experiments (Arzi 1978) and field studies (Hollister and Crawford 1986), but the grain-scale mechanisms of melt-induced weakening have been debated to the present day (e.g., Brown and Rushmer 1997; Rosenberg 2001). Renewed interest in synkinematic melting in recent years has stemmed primarily from two discoveries: first, seismic and magnetotelluric campaigns have detected partial melt within active orogens (Nelson et al. 1996; Schilling et al. 1997) usually at or near the base of thickened continental crust over areas of hundreds to thousands of km<sup>2</sup>. Second, numerical models of orogenesis show that the geometries of some orogens can only be reproduced if viscosity is reduced by an order of magnitude in at least a part of the lower, orogenic crust (e.g., Beaumont et al. 2001). Experiments on partially melted aggregates have shown that partial melting is the only viable mechanism for inducing such a marked drop in viscosity (e.g., Hirth and Kohlstedt 1995a, b).

These findings support the idea that melt-induced and -assisted flow is fundamentally important for the development of faults, structure, and topography at the orogenic scale.

In this chapter, we assess current knowledge of melt-induced effects on fault rocks and shear zone patterns. After reviewing experimental studies of deforming, melt-bearing rocks on the grain scale, we consider different approaches for obtaining estimates of melt content and residence time on different time and length scales in the continental crust. Numerical models of orogenesis indicate that the topography of mountain belts is inextricably linked to the presence or absence of melt-bearing rocks in the deep crust. We conclude with an outlook on possibly fruitful avenues of future research.

### EXPERIMENTAL DEFORMATION OF MELT-BEARING CRUSTAL ROCKS

A long-standing debate centers on the question of whether the reduction of rock strength with increased melt volume is exponential, linear, or is characterized by one or more discontinuities at specific melt volumes (Rosenberg and Handy 2005). The debate began when Arzi (1978) combined experimental strength data and

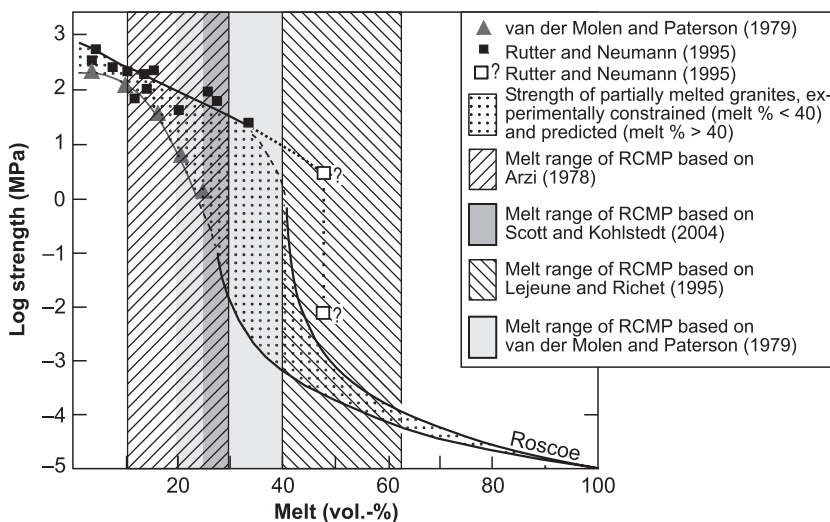


**Figure 13.1** Logarithmic strength versus melt volume % (modified after Rosenberg and Handy 2005). Open squares with question marks indicate a possible, but experimentally unconstrained range of strengths for samples containing 40% melt (Rutter and Neumann 1995). Continuous black lines show curves calculated from Roscoe’s (1952) equation for a suspension with grain-shape parameters used by Arzi (1978, left curve) and Lejeune and Richet (1995, right curve).

suspension theory to infer the existence of a dramatic strength drop within a critical range of volume percentages of melt (10–40%), termed the rheological critical melt percentage (RCMP, Figure 13.1). This strength drop was interpreted to coincide with a structural transition from a solid framework of crystals with interstitial melt pockets to a suspension of crystals in melt (Arzi 1978).

In Figure 13.2, we show that the available experimental data for deformed, partially melted aggregates can be fit by curves of exponential form, irrespective of the rock composition and starting texture in the experiments (aplite, granite, orthogneiss, amphibolite, experiments cited in the caption). The strength curves in Figure 13.2 are very steep at low melt volumes (<7 vol.-%), indicating that small changes in the amount of melt effect drastic changes of aggregate strength. At melt volumes greater than ~7%, all strength curves flatten, indicating a more moderate dependence of bulk strength on the amount of melt. The maximum change of slope of the exponential curves occurs at melt volumes of ~7%. The strength drop at melt volumes <7% appears to contradict previous work in silicates (Arzi 1978; van der Molen and Paterson 1979; Wickham 1987; Lejeune and Richet 1995; Scott and Kohlstedt 2004) and a variety of nongeological materials (compilation of Vigneresse and Tikoff 1999) claiming that strength drops most markedly at much higher melt volumes (20–50%, Figure 13.1).

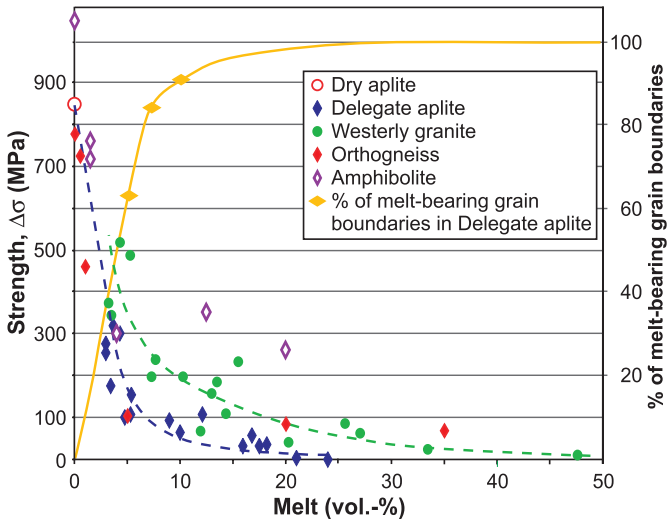


**Figure 13.2** Plot of strength versus melt volume % (modified from Rosenberg and Handy 2005). The experimental data are fitted by continuous curves. However, two straight lines intersecting at melt volumes of ~7% could also fit the data (Rosenberg and Handy 2005). Experimental data on delegate aplite is from van der Molen and Paterson (1979); westerly granite: Rutter and Neuman (1995); orthogneiss: Holyoke and Rushmer (2002); amphibolite: Rushmer (1995); dry aplite: Dell'Angelo and Tullis (1988).

It turns out that this discrepancy is not real, but only the result of the different scales used to plot the strength of the experimentally deformed aggregates. All previous authors plotted sample strength on a logarithmic strength scale (Figure 13.1) as a convenient way of depicting a strength decrease of more than four orders of magnitude at melt volumes between 20% and 50%, taken to be the RCMP. As shown in Figure 13.3, however, plotting strength on a linear scale reveals two strength drops: a large drop of ~800 MPa and nearly one order of magnitude at melt volumes between 0 and 6–7%, and a smaller drop of only a few MPa, but nearly 4 orders of magnitude at 20–50 vol.-% melt. This second drop is only visible in linear plots with an expanded lower end of the vertical axis (Figure 13.3). The first, larger strength drop does not correspond to a transition from a solid to a liquid suspension (solid-to-liquid transition of Rosenberg and Handy 2005; Figure 13.3), in the sense of the RCMP defined above. This conclusion relies first, on the relatively high (>100 MPa; Figure 13.2) differential stress that is still supported by the samples at melt volumes of 7%, suggesting the presence of a solid framework, and second, on the fact that solid aggregates collapse to form a suspension only if the liquid attains a minimum volume of 26% (e.g., van der Molen and Paterson 1979).

The more prominent first drop can be attributed to a transition from intragranular deformation of a crystal framework containing melt in isolated or partly connected pockets at 7 vol.-% to intergranular deformation of this framework within an interconnected network of melt film at 7 vol.-% (melt connectivity transition of Rosenberg and Handy 2005). Admittedly, this interpretation is speculative because the melt topology of the samples plotted in Figures 13.2 and 13.3 has not yet been investigated. However, microstructural analysis of the 3D melt network in sheared samples of olivine containing 7 vol.-% of metallic melt revealed interconnected melt films (Bruhn et al. 2000) within a continuous framework of solid grains. In addition, 80% of the grain boundaries of samples of Delegate aplite containing 7 vol.-% of melt were wetted by melt (van der Molen and Paterson 1979; Figure 13.2). At lower melt volumes, the percentage of grain boundaries wetted by melt showed a drastic decrease (Figure 13.2). Hence, the pronounced weakening at 7 vol.-% melt is interpreted to result from the concentration of deformation along interconnected, melt-bearing grain and phase boundaries within a solid aggregate (Rosenberg and Handy 2005). Hirth and Kohlstedt (1995a, b) attributed weakening of olivine aggregates deformed in the presence of basaltic melt primarily to the increased contact area of the melt along the grain boundaries, hence to the change in load-bearing area of the grain contacts. In addition, they showed convincingly that melting leads to an increase in the contribution of grain-boundary sliding during dislocation creep under constant load.

The extrapolation of these laboratory relations to natural rates and temperatures is problematic for several reasons: (a) the curves in Figure 13.2 are only

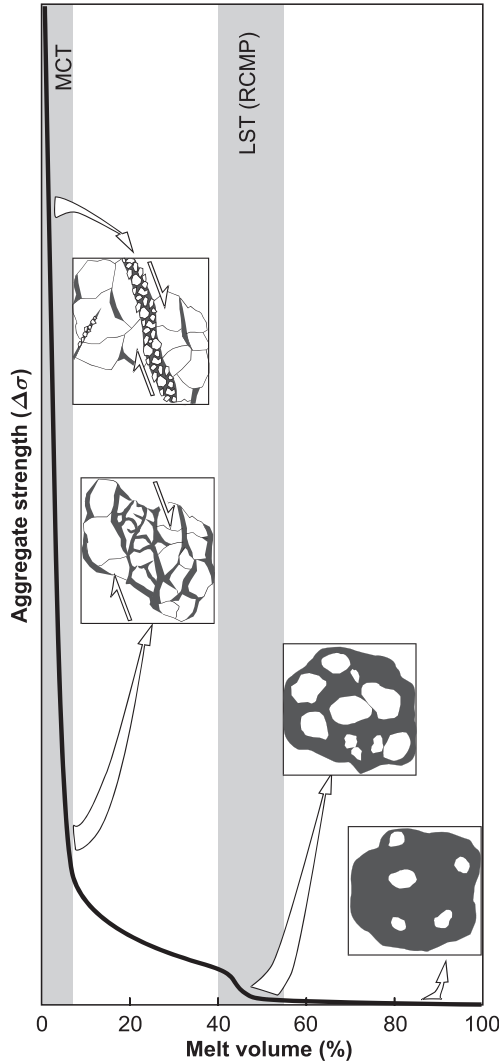


**Figure 13.3** Schematic plot of aggregate viscous strength versus melt volume % for silicate rocks between the liquidus and solidus (modified from Figure 4 in Rosenberg and Handy 2005). Note the two strength drops at the melt connectivity transition (MCT) and liquid-to-solid transition (LST); RCMP is rheological critical melt percentage. The vertical scale of the lower part of the ordinate is exaggerated to make the LST visible. The microstructural sketches illustrate deformation at different melt vol.-%. At 3 vol.-%, deformation localizes along a melt-bearing fault. At 7 vol.-%, deformation becomes more distributed, but is localized along the interconnected melt network on the grain scale. At 40–60 vol.-%, the solid crystal framework breaks down, but the grains still interact through the melt. Above 60 vol.-%, the solid particles suspended in the melt do not interact.

valid for the peak strength of samples at very small percentages of shortening (2–5%), not for flow strength at the high shear strains typical of natural deformation; (b) all experiments were performed in a closed system at undrained conditions (Renner et al. 2000), whereas natural deformation of melt-bearing rocks involves melt segregation and migration on a broad range of length scales (mm–km) indicative of drained conditions; (c) no reliable constitutive equation for melt-bearing crustal rock that includes melt volume percentage as an independent variable has been constrained yet on the basis of experimental data. Such flow laws are only available for olivine aggregates in the presence of small melt volume percentages (Hirth and Kohlstedt 2003; Zimmerman and Kohlstedt 2004). The paucity of experimental flow laws for anatectic aggregates reflects the basic difficulty of attaining steady state after only low strains in the laboratory. Moreover, cataclasis pre-empts creep due to the high melt pressures that accrue in undrained samples deformed at unnaturally high strain rates in the laboratory.

We note that the onset of melting may initially result in strengthening rather than weakening if water is partitioned from the crystals into the melt phase (Karato 1986). Water depletion hardens the creeping grains, as described for experimentally deformed olivine aggregates containing small percentages (<4%) of basaltic melt (Hirth and Kohlstedt 1996). However, this process, which is also inferred to be active in oceanic gabbros (Hirth et al. 1998), is limited to the onset of melting.

### **EXTRAPOLATION OF EXPERIMENTAL DATA TO NATURAL STRAIN RATES**

The laboratory experiments discussed above were performed at high strain rates ( $10^{-5}$ – $10^{-4}$  s<sup>-1</sup>), many orders of magnitude greater than natural creep rates. At the outset, we should like to point out a common source of confusion amongst experimentalists and structural geologists when discussing the extrapolation and application of laboratory results to nature: Experimentalists measure either stress at specified strain rate (creep tests) or strain rate as a function of applied stress (constant load tests), and then calculate the effective viscosity of the partially melted material. However, what counts from the perspective of tectonic modeling are viscosities as a function of melt content. For example, knowledge of effective viscosity allows modelers to calculate integrated crustal strengths. Historically, discussion on the mechanical properties of partially melted crust has been based on experimentally derived changes in sample strength as a function of melt content, without explicitly regarding viscosity during the experiments. Confusion has arisen because materials with different viscosities can support similar stresses while deforming at disparate rates in a crustal section. In the following, therefore, we

pay special attention to the viscosities of partially melted rocks in the rock-mechanical literature.

Despite the aforementioned difficulties of extrapolating laboratory results, there is evidence that the drastic change in the slope of the strength curves at melt vol. of 5–7% (Figures 13.2, 13.3) also pertains to changes in viscosity during natural deformation. So far, the only experimental flow law with direct application to anatexitic continental crust is for quartzite containing very low melt volumes (1–2 vol.-%, Gleason and Tullis 1995). Extrapolating the latter flow laws for both melt-bearing and dry (anhydrous, melt-free) quartzite to a natural strain rate of  $10^{-15} \text{ s}^{-1}$  indicates that the viscosity ratio of melt-bearing to melt-free quartzite decreases as temperature increases from 700 to 800°C (inset to Figure 13.4). At temperatures inferred to induce melting of pelitic rocks in the lower crust of the Himalayas (750–770°C; Patino Douce and Harris 1998), a melt volume of only 1–2% induces a viscosity drop of 25–30% (Figure 13.4). We note, however, that the differences in viscosities of melt-bearing and melt-free quartzite of Gleason and Tullis (1995) reflect contrasting activation energies with large errors as obtained in a deformation rig with a molten salt cell.

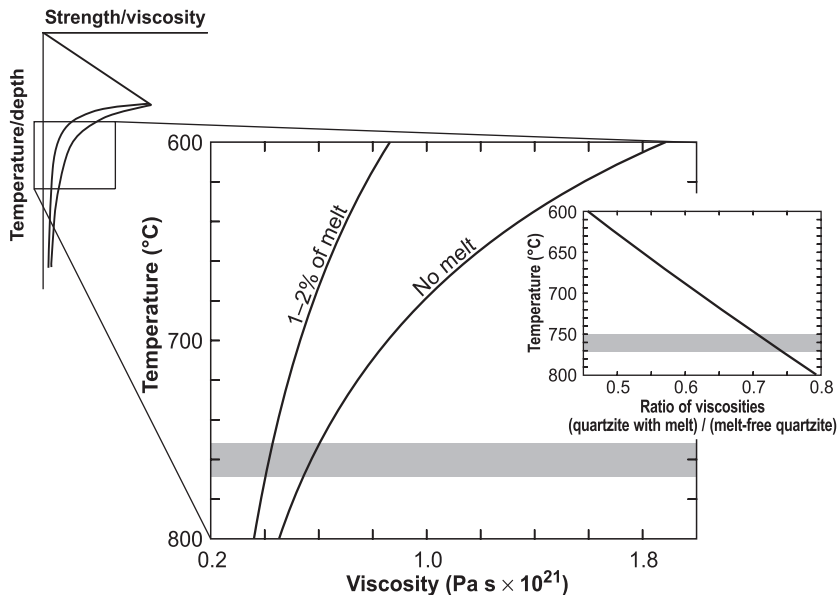


**Figure 13.4** Plot of viscosity of quartzite with 1–2 vol.-% of melt versus dry, melt-free quartzite for the temperature range 600–800°C obtained by extrapolating the flow laws of Gleason and Tullis (1995). Note in the inset the decrease in viscosity ratio with increasing temperature, suggesting that melt weakening is more dramatic at lower temperatures. Gray bar indicates the temperature range for crustal anatexis in the footwall of the South Tibetan detachment fault in Tibet (Patino Douce and Harris 1998).

Figure 13.5 shows a theoretical flow law derived by Paterson (2001; inset in Figure 13.5a) for diffusion-accommodated viscous granular flow in a closed system at melt volumes of 0 to ~20% (for a similar formulation see Rutter 1997).

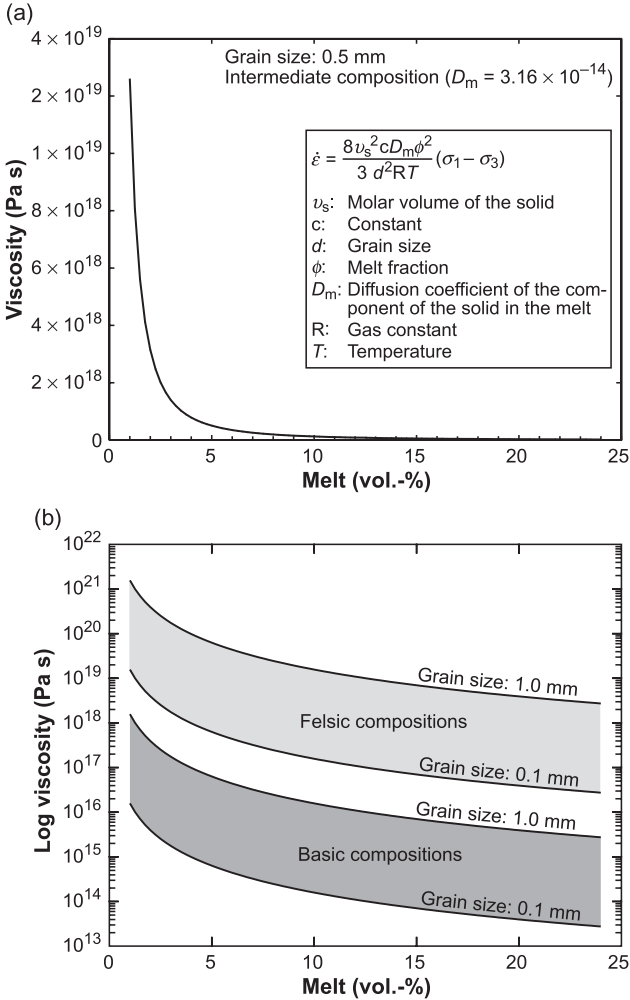


**Figure 13.5** Viscosity versus melt-volume % diagrams for the theoretically derived flow law of Paterson (2001). This flow law considers the diffusion of components between grains and melt, and therefore cannot be applied to the solid-state flow of materials (the effective viscosity becomes infinite if the melt vol.-% is 0). Thus, we only calculated the viscosity for melt volumes  $\geq 1\%$ . (a) Linear plot, for a rock of intermediate composition and grain size of 0.5 mm; see Paterson (2001) for the absolute values of parameters as a function of composition. (b) Log plot, showing the variation in viscosity as a function of grain size and composition.

This curve (Figure 13.5a), which indicates a power law relationship between viscosity and melt-volume percentage, reveals a dramatic change of slope at 3 to 4 vol.-% of melt (Figure 13.5a). The shape of this curve approximates the strength curves of experimentally deformed granite at slightly higher melt-volume percentages (Figures 13.2 and 13.3). Similar power law relationships between melt volume and viscosity apply variously to open systems that allow melt segregation, or to closed systems without melt segregation (Paterson 2001). The viscosity of melt-bearing granite in Figure 13.5a is calculated for a granitoid of intermediate composition and a grain size of 0.5 mm, which is a likely average for migmatitic crustal rocks. The effects of rock composition and grain size on the viscosity of the melt-bearing granitoid are shown on a log diagram in Figure 13.5b.

The available experiments on melt-bearing mantle rocks deformed in the diffusion creep and dislocation creep regimes without cataclasis, and to higher percentages of shortening (15–30%) than the granitoid samples of Figures 13.1 and 13.2, show an exponential decrease in viscosity with increasing melt volume (Hirth and Kohlstedt 2003; Figure 13.6). The viscosity of olivine drops dramatically, similar to the strength of experimentally deformed granite and the viscosity of granite calculated from Paterson's flow law.

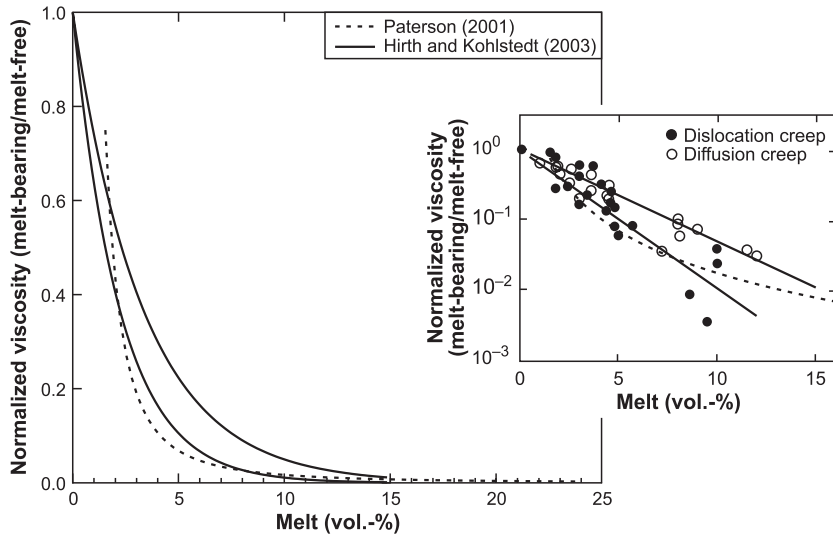


**Figure 13.6** Plot of viscosity versus melt volume % for olivine deformed in the presence of basaltic melt, modified from the logarithmic plot of Hirth and Kohlstedt (2003) shown in the inset. The viscosity is normalized to the viscosity of a melt-free aggregate deformed at the same conditions. Continuous curves represent the lower and upper bounds on the experimental data (see inset).

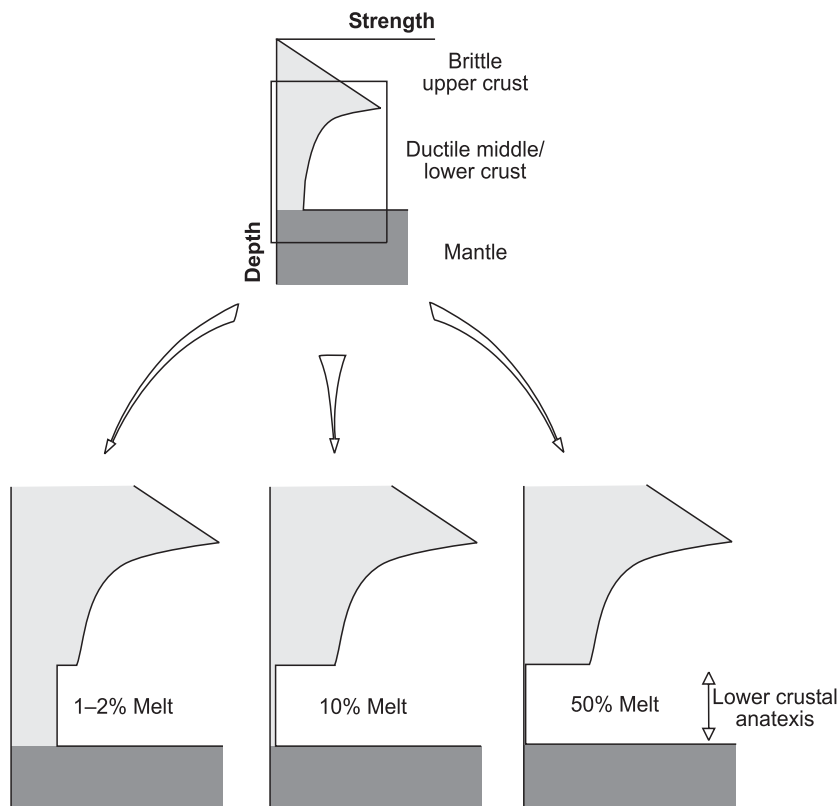


**Figure 13.7** Schematic strength profiles of continental crust containing a partially melted layer. The strength drop induced by 10 vol.-% melt is only marginally less than that induced by 50 vol.-%.

The consequence of experimental strength versus melt vol.-% relations for natural melt-bearing systems is visualized in Figure 13.7 in a series of schematic strength profiles for continental lithosphere containing a partially melted, lower crustal layer. These profiles suggest that the upper mantle is easily decoupled from the lower crust once the latter contains more than 7 vol.-% melt. Further melting (e.g., to 50 vol.-% at the solid-to-liquid transition), does not significantly change the structure and integrated strength of the lithosphere (Figure 13.7).

In the following sections of this chapter, we test the validity of the strength profiles in Figure 13.7, first by considering the relationship between estimated present-day melt content and the topography of Tibet, and second by considering the amount of melt-induced weakening necessary to reproduce the geometrical characteristics of orogens in numerical models.

## ESTIMATES OF MELT CONTENT AND RHEOLOGICAL TRANSITIONS IN NATURE

Estimates of melt volume in anatexitic rocks from exhumed orogens range from 10 to 40 vol.-% (Teyssier and Whitney 2002). However, small amounts of melt (= 5 vol.-%) are probably overlooked in crustal rocks, especially if the melt did not segregate into discrete leucosome lenses. Indeed, several microstructural investigations have reported such small melt percentages (e.g., Sawyer 2001; Marchildon and Brown 2002). In addition, the estimates above cannot tell us whether all of the melt inferred from measurements at the outcrop scale was present in the rocks at the same time.

Real-time distribution of partial melts at depths of more than 20 km beneath the Puna part of the Andean Plateau and Tibetan Plateau have been inferred from anomalies in seismic attenuation (the ratio of P-wave to S-wave velocities, Nelson et al. 1996; Yuan et al. 2000) and electrical conductivity (Schilling et al. 1997; Li et al. 2003; Schmitz et al. 1997; Unsworth et al. 2005). These anomalies have been interpreted to be melt-bearing layers that extend horizontally over hundreds of km and with thicknesses varying from 10 to 40 km (e.g., Nelson et al. 1996; Gaillard et al. 2004). This interpretation is consistent with the inferred temperatures of 700°C at 18 km depth and 800°C at 32 km depth below Tibet, based on the seismically derived depth of the  $\alpha$ - $\beta$  transition in quartz (Mechie et al. 2004). As shown in Figure 13.6, dehydration melting in the Himalayan crust takes place at 750°C (Patino Douce and Harris 1998). Recent magnetotelluric investigations suggest that the melt content below Tibet is not more than 5–14 vol.-%, and may be as small as 2–4 vol.-% below the northwestern part of the Himalayas (Unsworth et al. 2005). By assuming that melt-bearing rocks are porous elastic media on the time scales of the geoelectric measurement, Schilling and Partzsch (2001) used the conductivity results to calculate a melt volume of at least 20% below the Puna and the Tibetan Plateaus.

These estimated melt volumes are consistent with a viscous strength drop of ~15 times below the Puna Plateau and ~10 times below the Tibetan Plateau according to the strength versus melt vol.-% relations compiled in Figure 13.2. As shown below, thermomechanical models of orogenesis require an order-of-magnitude drop in viscous strength within the lower crust to develop orogenic plateaus (Beaumont et al. 2001). In this context, it is interesting to note that the Tibetan Plateau overlies crust containing 5–14 vol.-% melt, whereas only 2–4 vol.-% melt underlies the northwestern part of the adjacent Himalayas (Unsworth et al. 2005). This change in melt content coincides with the range of melt volumes marking the transition from the melt connectivity transition to the more flat-lying part of the strength curve in experimentally deformed, melt-bearing granitic rocks (Figure 13.3). Therefore, we infer that it coincides with a major transition in the integrated strength of the crust. If so, then small amounts of melt may be the prime factor governing variations in plateau topography.

The higher end of the range of melt contents in exhumed anatectic rocks (30–40 vol.-%) corresponds to the liquid-to-solid transition in Figure 13.3 (Rosenberg and Handy 2005; RCMP of Arzi 1978). The liquid-to-solid transition also corresponds to the transition from metatexite to diatexite in partially melted rocks and has been interpreted as the fundamental rheological transition within the ductile part of the continental crust (Vanderhaeghe and Teyssier 2001a). These authors argue that the formation of diatexites at melt volumes as high as the SLT controls the formation of migmatite-bearing domes in the North Canadian Cordillera by weakening the crust to a point that allows the onset of gravitational collapse. We consider this unlikely, however, given that the contact between metatexite and diatexite in these domes does not coincide with any marked structural discontinuity in the sense of a shear zone (Vanderhaeghe and Teyssier 2001a, their Figure 4). These observations reinforce our opinion that the melt connectivity transition is far more important than the liquid-to-solid transition from a rheological standpoint. If indeed melt volumes in natural systems reach 30 to 40 vol.-% at the liquid-to-solid transition, then this results in a comparatively modest drop in strength. To our knowledge, systematic changes of structural style related to variations in viscous strength as a function of melt content have yet to be described in naturally deformed anatectic rocks.

### **RESIDENCE TIME OF MELT IN OROGENIC CRUST**

The rate and time to produce and maintain a rheologically critical amount of melt (= 7 vol.-% at the melt connectivity transition in Figure 13.3) govern the effect of melting on faulting in the lithosphere. Melting times are poorly constrained, partly because this time varies with the volume of melt considered and partly because melting rates are not well known. A minimum melt time of  $10^5$  years is obtained from studies of plutons (compilation of Petford et al. 2000). An upper limit for the residence time of melt in orogenic crust can be estimated by relating the extensive layers of geophysically imaged, melt-bearing crust beneath the Andean and Tibetan Plateaus to the ages of exposed magmatic bodies inferred to have formed by melting of these layers. Magmatic activity in the northern, Altiplano part of the Andean Plateau started in Miocene time some 23 Ma ago and has continued unabated to the present (de Silva 1989), leading to the formation of a large ignimbritic complex. Dacitic volcanism in the more southerly Puna part of the plateau started at 10 Ma and continued until 2 Ma (Riller et al. 2001). The melt feeding this volcanism is still present in a partially melted layer at 20–25 km depth, as determined by the geophysical studies cited in the previous section (e.g., Yuan et al. 2000). The residence time of melt beneath the Andean Plateau is therefore at least 10 Ma, possibly as much as 23 Ma.

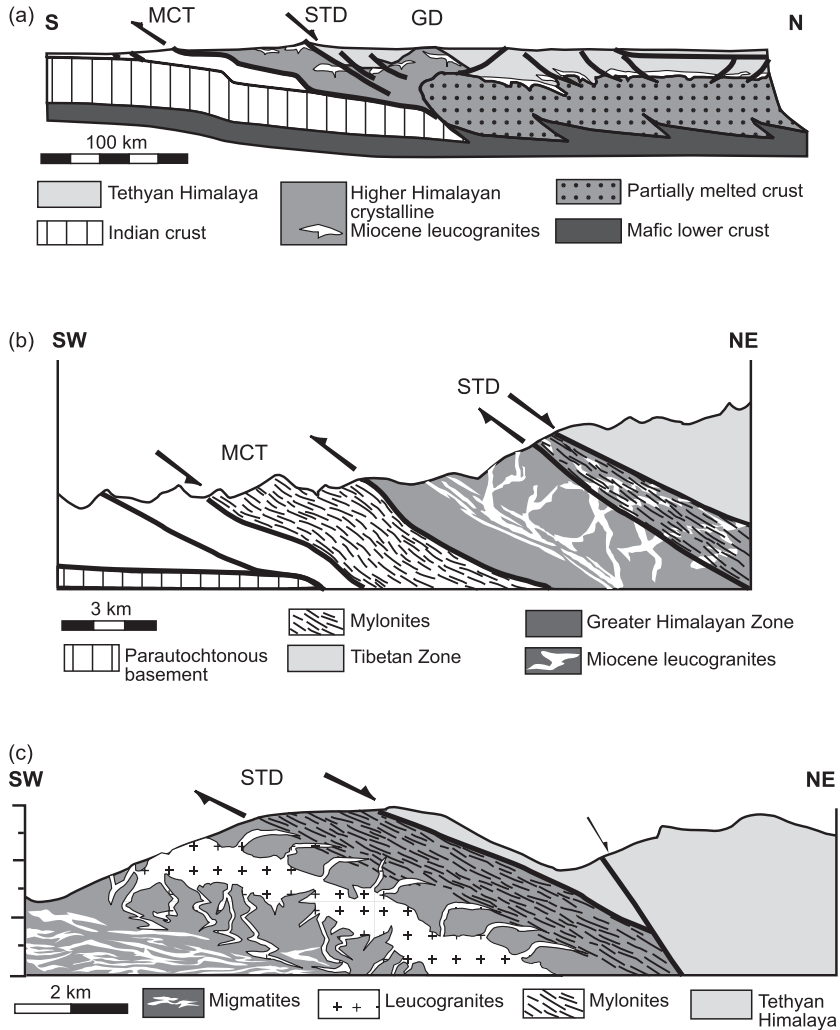


**Figure 13.8** Cross sections of the Tibetan-Himalayan orogen. MCT: Main Central Thrust, STD: South Tibetan detachment, GD: gneiss domes. (a) INDEPTH profile, modified from Nelson et al. (1996). The partially melted region is inferred from seismic data. (b) Cross section of the Annapurna area in the Himalayas, modified from Hodges et al. (1996). Note that leucogranites are concentrated in the central part of the High Crystalline Complex, not along the South Tibetan detachment. (c) Cross section of the STD, in the Northwest Himalayan (Zaskar), modified from Dèzes et al. (1999). Migmatites concentrate well below the extensional mylonites of the STD, confirming the observations of the Annapurna section. Leucogranitic plutons are located well below the detachment and are only marginally affected by mylonitic deformation.

The melt imaged below the Tibetan Plateau may be related to a chain of leucogranite bodies situated in the footwall of a large (>1000 km length) low-angle normal fault, the South Tibetan detachment system (Figure 13.8 and discussion in section below on FIELD-BASED MODELS OF THE EFFECTS OF MELT ON LARGE-SCALE FAULT ZONES). These granites range in age from 24 to 10 Ma (e.g., Zhang et al. 2004), most of them from 22 to 19 Ma (review of Searle and Godin 2003). Some authors claim that these leucogranites are continuous with the partially melted intracrustal layer imaged below the Tibetan Plateau (e.g., Nelson et al. 1996; Wu et al. 1998; Fig. 13.8). If so, the lower crust of Tibet has been partially molten for more than 20 Ma, similar to the maximum residence time of melt in the lower crust of the Andean Plateau. This long time interval covers a significant part of the uplift history, which probably started in latest Cretaceous to Early Tertiary time in the Tibetan region (Yin and Harrison 2000) and in Early Tertiary time in the Andes (e.g., Lamb et al. 1997). Dating of synkinematic leucosomes in anatexitic rocks of older orogens (e.g., Variscides: Brown and Dallmeyer 1996) also shows that melt may have been present in the crust for similarly long times.

The long residence times of melts beneath orogenic plateaus contrast with the much shorter times of melts in steeply-dipping shear zones and faults (= 1.5 Ma; e.g., Davidson et al. 1992; Oberli et al. 2004). As discussed below, these short residence times can lead to transient motion (Handy et al. 2001).

### **FIELD-BASED MODELS OF THE EFFECTS OF MELT ON LARGE-SCALE FAULT ZONES**

Melt-induced weakening of the crust is expected within subhorizontal, lower crustal layers for the simple reason that—barring decompression melting during rapid exhumation—isothersms at or near the solidus are generally subhorizontal. Shear zones engendered by melt-induced weakening at depth form decoupling horizons within the lithosphere, but their long-term effect on the bulk rheology of the lithosphere is expected to depend on their geometry as well as on the regional stress field. For example, most strike-slip faults are steeply inclined and transect melt-bearing layers at larger angles than thrusts and normal faults. Whereas thrusts and normal faults may root in weak, melt-bearing layers, strike-slip faults are more likely to serve as conduits for the channeled ascent of melts to higher crustal levels (e.g., D’Lemos et al. 1992; Handy et al. 2001) where they crystallize rapidly (e.g., Davidson et al. 1992). In the following, we examine some of the controls on melt-enhanced shearing and lithospheric rheology.

## **Transpressive Settings**

### *Historical Perspective*

Hollister and Crawford (1986) were the first to argue that there is a causal relationship between large-scale deformation and melting in orogenic crust. They proposed that melting weakens the lower crust significantly during orogenesis, thereby increasing strain rates there and augmenting the exhumation rates of crustal blocks confined between melt-bearing shear zones. These enhanced displacements were termed “tectonic surges.” Their existence was posited mainly on the following observations: (a) Crustal rocks weaken significantly upon melting, as shown in experimental deformation of partially molten aggregates; (b) There is a close spatial relationship between sites of large deformation (shear zones) and the occurrence of migmatitic or magmatic rocks, for example, in the Coastal Mountains of British Columbia; (c) Rapid decompression (exhumation) in the Coastal Mountains coincided with the thermal peak of metamorphism, which induced partial melting.

Whether or not melting of lower crust is necessary to attain such rapid exhumation rates is questionable. Since Hollister and Crawford’s (1986) landmark paper, exhumation rates much higher than those they reported ( $1 \text{ mm yr}^{-1}$ ) have been documented in several orogens that lack visible evidence of melted crust (e.g., Milliman and Syvitski 1992). The coincidence of high exhumation rates in crustal blocks with the occurrence of melt in adjacent shear zones does necessarily mean that melt was the main agent of the increased rates of exhumation.

Numerous field-based investigations of large-scale transpressive fault systems have demonstrated the close spatial relationship between migmatites and/or magmatic rocks and mylonitic shear zones (e.g., Davidson et al. 1992; D’Lemos et al. 1992; McCaffrey 1992; Hollister 1993; Ingram and Hutton 1994; Tommasi et al. 1994; Berger et al. 1996; Neves et al. 1996; Vauchez et al. 1997; Tikoff and de Saint-Blanquat 1997; Brown and Solar 1998). All these studies established that mylonitization occurred in the presence of melt. Thus, shear zones were believed to nucleate in the melt-bearing crust and propagate into thermally weakened country rocks (Neves et al. 1996).

Unfortunately, field observations alone are insufficient to discriminate between melt-induced localization of deformation and deformation-induced melt channeling, because the structural evidence of both processes is probably the same, viz., the occurrence of granite in shear zones. The fact remains that the available criteria are equivocal, as pointed out by Vauchez et al. (1997) and discussed below.

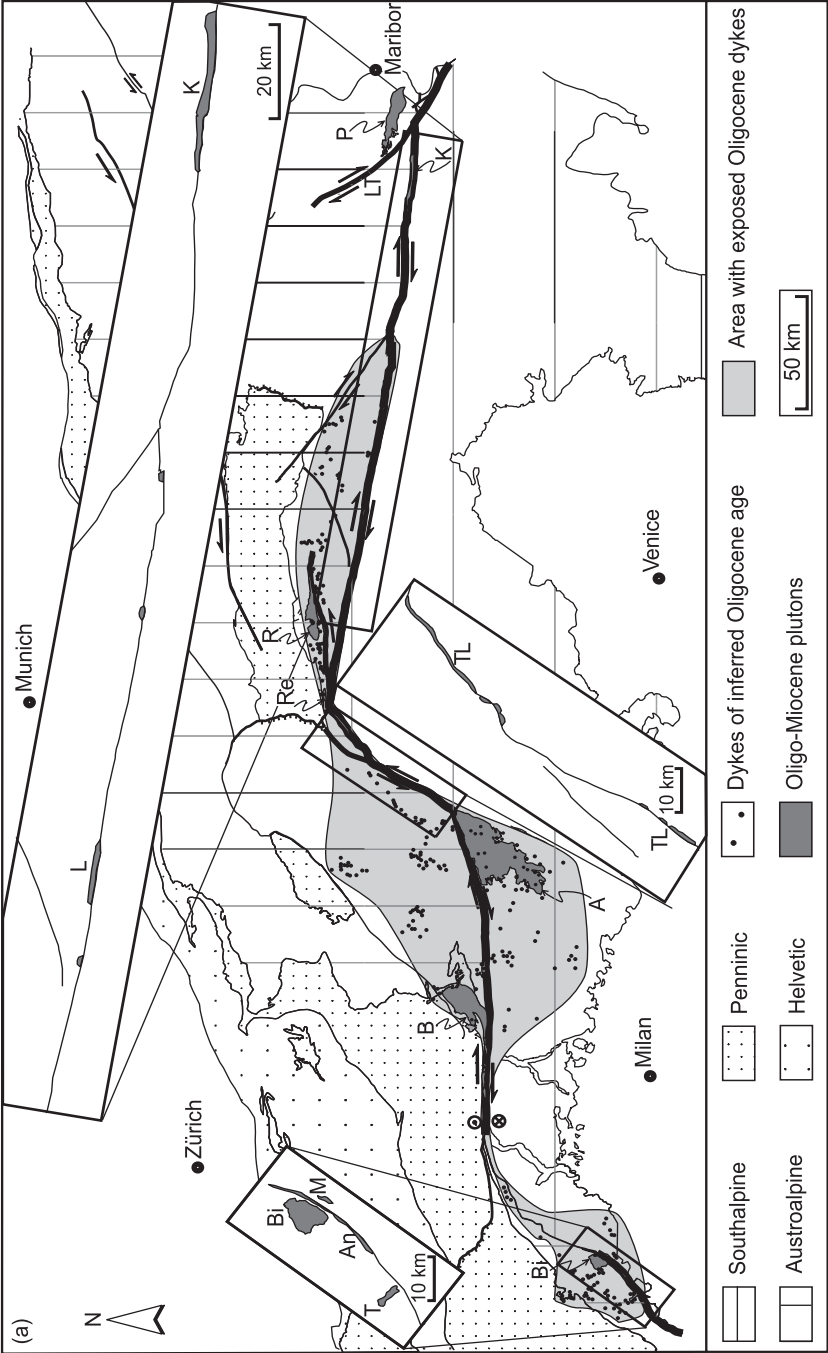
### *Tertiary Plutonism in the Alps*

The dextral transpressive Periadriatic fault system in the Alps is closely associated with Late Oligocene plutons (Figure 13.9a) whose source region is inferred

to be the base of the thickened Alpine orogenic crust (von Blanckenburg et al. 1998). The Periadriatic fault system extends from the surface down to the top of the lower, mafic crust as shown in geophysical transects (Schmid and Kissling 2000). All plutons exposed adjacent to the Periadriatic fault system crystallized within a restricted time interval of approximately 5 Ma during a broader period of fault activity (review in Rosenberg 2004). The exhumation of crustal levels from the surface down to 25–30 km allows a unique reconstruction of the geometrical relationships between magmatic bodies and shear zones in profile, as shown in Figure 13.9b. This reconstruction shows that magmatic bodies accompany the fault plane almost continuously from the surface to the maximum paleodepth of 25–30 km and possibly beyond, whereas no intrusive bodies occur away from the fault plane (Figure 13.6b). Thus, the plutons ascended along the Periadriatic fault system.

Isotopic ages showed that the base of the Bergell tonalite (marked B in Figure 13.9a) at a paleodepth of ~25 km (Figure 13.9b) remained in a partially molten state for at least 1.5 Ma (Oberli et al. 2004) within the mylonitic belt of the Periadriatic fault system. In contrast, the close similarity of ages obtained by isotopic systems with different closing temperatures on upper crustal ( $\leq 10$  km depth) plutons such as the Biella Pluton (Western Alps, Italy; Figure 13.9a) and Adamello (Southern Alps, Italy; Figure 13.9a) indicates rapid crystallization. Therefore, the effect of melt on deformation is expected to depend strongly on the level of melt emplacement, and hence on the melt residence time. 1.5 Ma is probably an upper time limit for the existence of melt in a pluton that is ascending as an elongate sheet along a fault plane. This factor represents a fundamental limitation to the process of melt-weakening in transpressive systems. Once the melt crystallizes, the pluton plus its host shear zone are expected to harden (Handy et al. 2001).

We emphasize that the close spatial and temporal relationship between plutons and the Periadriatic fault system (Figure 13.9a) does not result from melt-induced strain localization, but rather from deformation-induced channeling of melts into an active, orogen-scale fault system (Rosenberg 2004). The fault rocks of the Periadriatic fault system overprint first-order Mesozoic paleogeographic and Alpine metamorphic boundaries that have been interpreted as the sites of repeated transform, strike-slip motion in Jurassic and Late Cretaceous times (Schmid et al. 1989, Froitzheim et al. 1996), long before Tertiary intrusive activity and differential exhumation of the plutons affected the retrowedge of the Tertiary Alpine orogen. Moreover, numerical models of the Central Alps indicate that an orogenic retrowedge bounded by a steep backthrust like the Periadriatic fault system in the central to western part of the Alps develops in kinematic response to a subduction singularity irrespective of the presence of melts and of numerous rheological heterogeneities (Schmid et al. 1996). If the present exposure of minor Tertiary dykes that are geochemically related to the plutons (Figure 13.9a) is taken as a first-order proxy for the areal extent of the



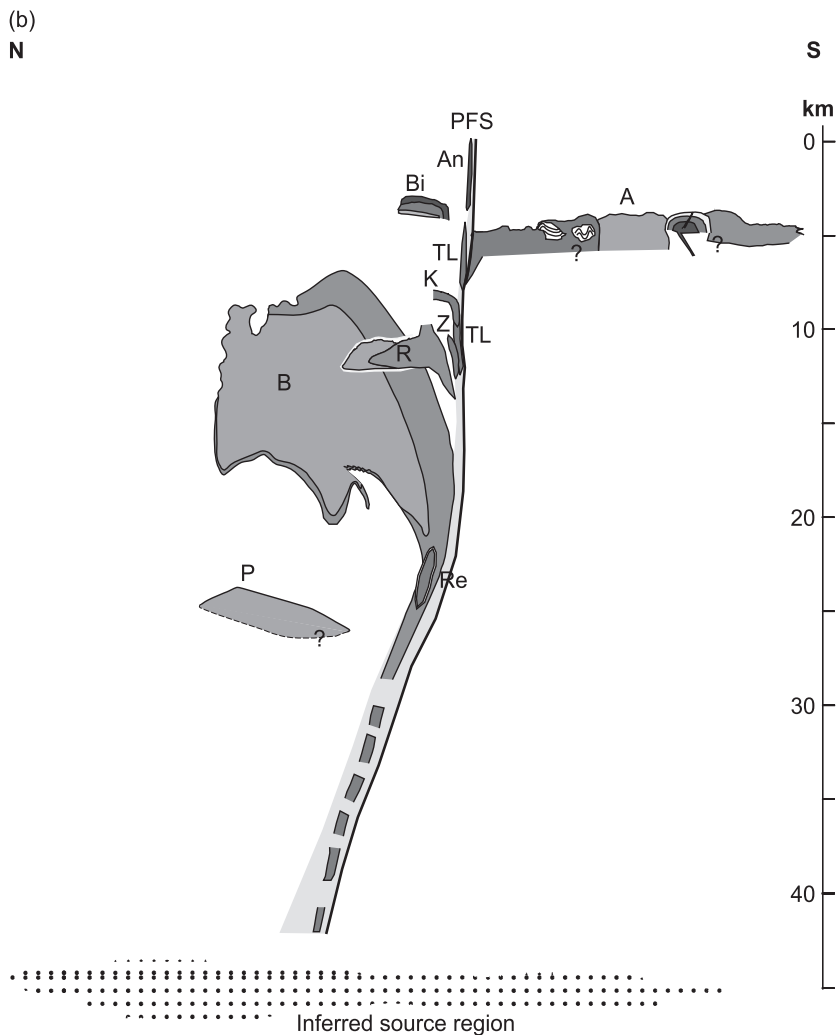


**Figure 13.9** Plutons along the Periadriatic fault system of the Alps. *Facing page:* (a) Simplified tectonic map of the Alps showing the major Tertiary faults and shear zones, the Oligo-Miocene plutons, and locations of Tertiary dykes (modified from Rosenberg 2004). Periadriatic fault system is shown with thick black lines. Boxed areas contain detailed maps of thin magmatic sheets along the Periadriatic fault system. *Above:* (b) Synthetic cross section showing the relationship of the Periadriatic fault system (PFS) to the plutons at their original depths of emplacement (modified from Rosenberg 2004). The depth and distance of each pluton from the Periadriatic fault system are constructed from geobarometric and field data. A: Adamello Batholith; B: Bergell Pluton; Bi: Biella Pluton; K: Karawanken Pluton; P: Pohorje Pluton; R: Rensen Pluton; TL: Tonalitic Lamellae; Z: Zinsnock Pluton.

underlying melt source, then the concentration of the synkinematic feeders of the intrusive bodies within the 2–3 km wide mylonites of the Periadriatic fault system gives a good impression of the degree to which upward melt flow was channeled parallel to the steep mylonitic foliation.

### *Magmatic Arcs*

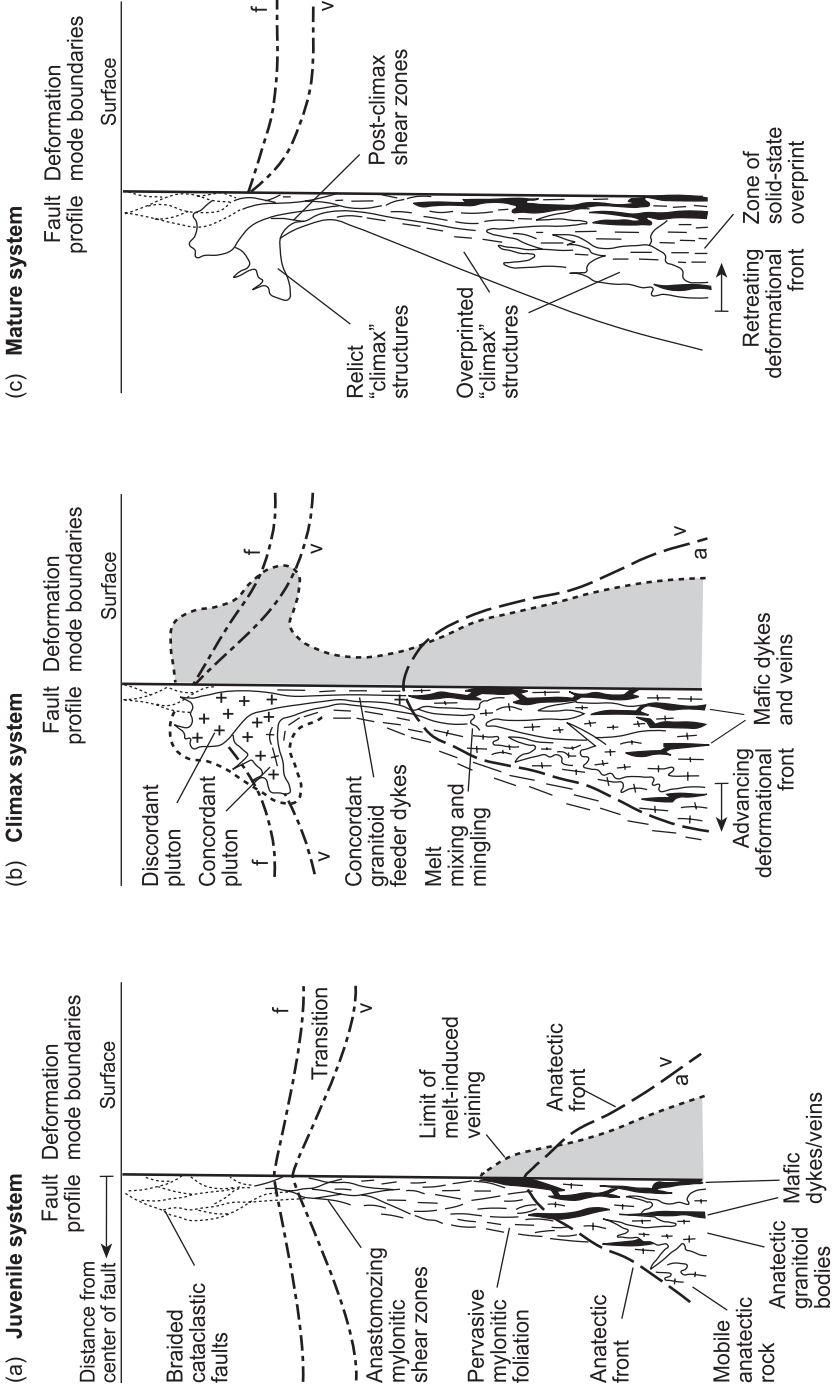
Arc-parallel strike-slip faulting (e.g., Jarrard 1986) is thought to result from strain partitioning of overall oblique convergence into a steep zone of predominantly simple shear flanked by domains of more distributed pure shear (e.g., Teyssier et al. 1995). Besides the obliquity of convergence, crustal strength is an important control on this strain partitioning. Several authors have pointed out the obvious relationship between arc-parallel strike-slip faults and magmatic arcs, which are interpreted as zones of crustal weakness due to the high thermal gradients associated with the advection of heat from melts (e.g., Jarrard 1986; Scheuber and Andriessen 1990). Melt-induced weakening may explain why strike-slip faulting is very common in the upper plate of ocean–continent subduction systems (de Saint-Blanquat et al. 1998), whereas only one fifth of upper oceanic plates in ocean–ocean subduction systems have such structures (Jarrard 1986). This holds true even in subduction systems with high convergence angles (e.g., Sumatra: 50°, Andes: 60–90°), in other words, at angles that do not favor partitioning in the absence of melting. A case in point is South Island, New Zealand, where active magmatism is absent and no strike-slip partitioning occurred, in spite of the highly oblique convergence (16–29°; de Saint-Blanquat et al. 1998, and references therein). Note however, that weakening of the crust, leading to the partitioning of deformation along arc-parallel strike-slip faults may not only result from the presence or absence of melt, but from the occurrence of older anisotropies, as suggested for the Taiwan subduction system (Fitch 1972), or by stronger erosion in the retrowedge of the accreted crust, which may allow the lateral and the convergent components of strain to occur both on the same fault plane, as inferred for South Island (New Zealand; Koons et al. 2003). The geometry of the melt bodies presumed to be responsible for weakening at depth within magmatic arcs is unknown. Several studies have noted a positive correlation between the intensity of magmatism (volume of melt generated per time) and the obliquity of convergence (Western USA: Glazner 1991; Andes: Günther 2001). This was thought to result from the intrusion of melt into secondary extensional structures at releasing bends along the strike-slip faults (Glazner 1991; McNulty et al. 1998). If so, then transcurrent deformation is the cause for the spatial and temporal association of faults and plutons. This contrasts with the idea propounded above that melt induces the partitioning of deformation by reducing the viscous strength of the crust within the arc.

*Positive Feedbacks between Melting and Faulting*

Different opinions on the cause and effect of strain localization in melt-bearing crust have been reconciled by the idea that deformation and melt interact in a positive feedback loop. De Saint-Blanquat et al. (1998) suggested that magma ascent induces localization of deformation into strike-slip faults, which in turn create the space for melt ascent, which further weakens the crust and hence reinforces localization of deformation into the strike-slip zone. A slightly different process was described for intracontinental settings by Brown and Solar (1999), who pointed out that transpressive deformation on the orogen-scale leads to an upward displacement of the isotherms (e.g., Huerta et al. 1996), which creates an antiformal thermal structure. This structure can be amplified, if heat is advected by ascending melts, thus extending the zone of deformation upward, which in turn favors the upward migration of melts in a positive feedback loop (Brown and Solar 1999).

Positive feedbacks during a single magmatic cycle are depicted in the series of sections through a generic strike-slip fault in Figure 13.10, following Handy et al. (2001, their Figure 11). Incipient melting at depth (juvenile stage, Figure 13.10a, d) thermally weakens the lower crust, increasing the strain rate and loading shallower crustal levels of crust that undergo solid-state creep and frictional sliding. Together with the accumulation of large bodies of segregated melt, this favors melt-induced upward veining which facilitates the rapid, buoyant rise of melt within the fault system (climax stage in Figure 13.10b, e). During this stage, the rise of the isotherms (e.g., Huerta et al. 1996) combined with the presence of low-viscosity melt in veins connecting plutons with their source regions at depth act to accelerate fault movement. For example, Davidson et al. (1992) has estimated that a km-thick syntectonic tonalite within the McLaren Glacier metamorphic belt in Alaska accommodated at least 10 km of displacement within an estimated time to crystallization of only 90,000 years. Mature fault zones (Figure 13.10c, f) are expected to harden as the melts within them crystallize, the isotherms subside, and the geotherm decreases. In fact, mature fault zones can attain an integrated strength greater than their pre-melting strength if the crystallized melts (e.g., mafic melts) have greater solid-state creep strengths than the rocks they displaced during intrusion.

The model in Figure 13.10 suggests that the feedback between deformation and magmatism in oblique-slip fault systems may induce cyclical weakening-then-hardening of the continental crust on time scales of only  $10^3$ – $10^5$  years (Handy et al. 2001). This is much shorter than the total duration of motion ( $10^6$ – $10^7$  years) along the plate boundaries in which the faults occur. We have pointed out before that episodic melt-induced fault slip may be responsible for repeated, sudden shifts in sedimentary depocenters and volcanic fields along the margins of basins bounded by oblique-slip faults (examples in Biddle and Christie-Blick 1985).



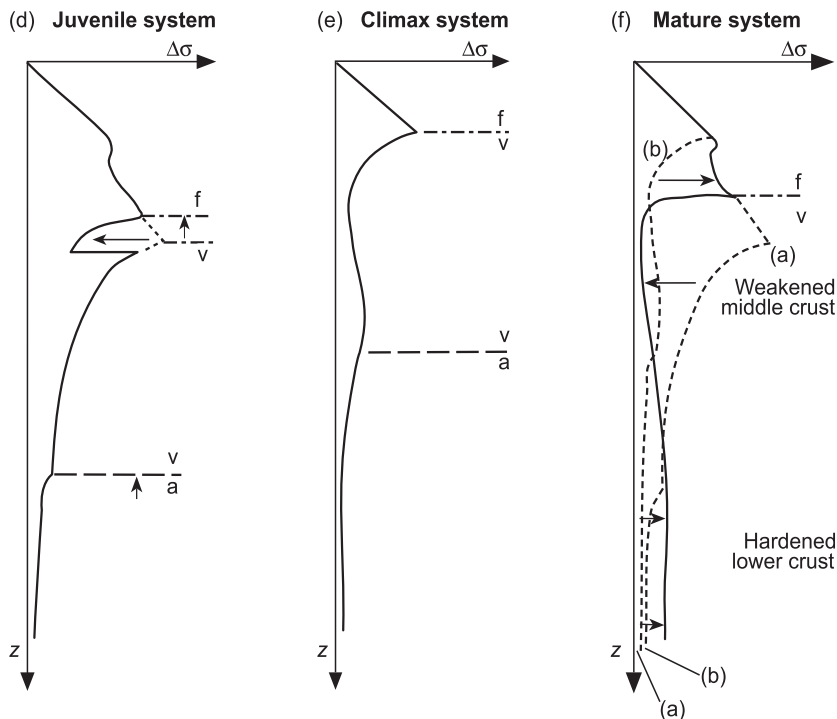


**Figure 13.10** Facing page: Structure and strength versus depth diagrams for a generic strike-slip fault zone undergoing one cycle of syntectonic magmatism (modified from Fig. 11 of Handy et al. 2001). Structure versus depth diagram is shown for (a) the juvenile, (b) climax, and (c) mature stages. The dashed-dotted curves represent the frictional-viscous (f-v) transition; dashed curve is the transition from solid-state viscous creep (marked v) to melt-assisted viscous granular flow (anatectic flow, marked a); the dotted curve is the limit of melt-induced veining (gray area on right-hand side of the diagram). The figure depicted above shows strength versus depth diagrams for (d) the juvenile stage, (e) the climax stage, and (f) the mature system stage. Bold dotted lines in (f) depict the strength profiles during previous stages; arrows indicate movements of curves since these stages.

## Syn-orogenic and Post-orogenic Extensional Settings

### Historical Perspective

Wernicke et al. (1987) were the first to note a systematic relationship between the onset of crustal extension and the amount of Late Cretaceous–Early Tertiary plutonism in the North American Cordillera. Areas where extension initiated earliest (55–49 Ma) have the largest volumes of intrusive rock compared to other areas where extension began later (38–20 Ma, minor intrusive rocks),

or only ~15 Ma ago (no intrusive rocks). They proposed that extension results from gravitational spreading of the previously thickened lithosphere and that extension initiated in the partially melted lower crust with the attainment there of the rocks' melting temperature, as previously suggested by Coney and Harms (1984). In this interpretation, the low-melt viscosity was not considered to be the direct cause of crustal weakening, but instead melt was interpreted to indicate high temperature, hence thermal weakening of the lithosphere. The close spatial and temporal relationship between magmatism and extension in the North American Cordillera was later corroborated by the synthesis of an immense set of structural and geochronological data covering western North America from Alaska to Mexico (Armstrong and Ward 1991). In contrast to Wernicke et al. (1987), Armstrong and Ward (1991) recognized that melt drastically reduces the viscosity of the crust due its own very low viscosity, in addition to thermal weakening of its solid host rocks. They suggested that melt-induced weakening triggered extension of previously thickened crust. This idea has since been used to explain coeval melting and extensional deformation in Tertiary orogens such as the Tibetan Plateau (e.g., Burchfiel et al. 1992; Hodges 1998), the Hellenides (Vanderhaeghe and Teyssier 2001b), as well as in older orogens like the Variscides (Vanderhaeghe et al. 1999) and the Caledonides (e.g., McLelland and Gilotti 2003).

In the following, we refer to gravitational collapse as "gravity-driven ductile flow that effectively reduces lateral contrasts in gravitational potential energy" (Rey et al. 2001). As shown by Willett and Pope (2004) this process may be transient. Absent any changes in tectonic forces, the critical parameter controlling gravitational collapse is the ratio of the gravitational load to the strength of the crust (Rey et al. 2001). Therefore, weakening the crust by partial melting can trigger such collapse. Structural and geochronological evidence for coeval extensional faulting and magmatism supports, but does not prove, the hypothesis that melting triggers gravitational collapse. Orogenic modeling has shown that both extensional faulting and crustal anatexis may be triggered by other tectonic processes (e.g., loss of a dense, isostatically unstable root or a subducting slab; Houseman et al. 1981). Thus, in some tectonic settings neither process causes its other, but both may have a common cause.

If the onset of extension systematically postdates the onset of melting within a short time interval, then melting may be inferred to trigger gravitational collapse. However, establishing such a causal relationship is beset with the basic problem that extension is commonly dated with crystallization ages of synkinematic migmatites (e.g., Dèzes et al. 1999). Thus derived, the radiometric ages of extension and melting are obviously not independent. Given the duration of magmatic events (~ $10^7$  years, see below) during the late stages of orogeny, it is unreasonable to assume that minerals from anatectic leucosome provide anything more than "snapshot" ages of their crystallization during a much longer-lived event.

Likewise, but on a much larger scale, cross-cutting relations between shear zones and intrusive bodies only tell us locally which structure formed first, not whether these structures formed at the very beginning or late in the history of shearing and intrusion, much less which process (shearing or intrusion) started first. Mutually cross-cutting relationships can be interpreted to show that two events were broadly coeval in a given rock volume, but they do not indicate which event began first.

### *Melting and Syn-orogenic Extension in the Himalayas*

The relationship between melting and normal faulting along the South Tibetan detachment system in the Himalayas (STD, Figure 13.8) is the subject of ongoing debate. Some authors infer that crustal melting, which engendered the Miocene leucogranite bodies in the footwall of the STD, resulted from isobaric decompression during extension (Harris and Massey 1994; Dèzes et al. 1999; Harris et al. 2004). Based on thermal modeling, others consider that extensional decompression is unlikely because it requires extremely rapid ( $= 20 \text{ mm yr}^{-1}$ ) and large-magnitude denudation to produce minor amounts of melt, and because the ages linking slip on the normal faults with melting are not well constrained (Harrison et al. 1999). The latter authors invoke shear heating along the Main Central Thrust (MCT in Figure 13.8; Le Fort 1975; England et al. 1992) as the main heat source for partial melting.

At a very basic level, the debate is fueled by ambiguous field relations. Parts of the STD are truncated by leucogranitic bodies (e.g., Guillot et al. 1994; Edwards et al. 1996) which are themselves deformed by brittle normal faults in the hangingwall of the STD (Brown and Nazarchuk 1993). Some of the granites that intrude the STD have very young ages (12.5 Ma; Edwards and Harrison 1997), which clearly postdate the oldest (late Oligocene) crystallization ages of kyanite-bearing leucosomes in the inferred source region of the leucogranites at the base of the High Himalayan Crystalline Complex (Hodges et al. 1996). In other localities extensional shear zones of the STD overprint the leucogranite (Searle and Godin 2003). Thus, both melting and deformation persisted for several Ma (Searle and Godin 2003; Hodges et al. 1996).

Th-Pb dating of monazites (Kohn et al. 2005) suggests that the MCT initiated as recently as  $16 \pm 1 \text{ Ma}$ , earlier than the inferred age of some (but not all) leucogranitic plutons along the STD. Additional complexities arise from recently obtained Oligocene ages (27.5 Ma) of Himalayan plutons north of the STD (Zhang et al. 2004). The composition of these granites indicates that they were derived from the same melt source as the Miocene leucogranites (the High Himalayan Crystalline Complex), but at greater depth. If the Oligocene ages reflect the onset of melting in the High Himalayan Crystalline Complex, then melting definitely initiated before extension along the overlying STD and, indeed, may have triggered this extension. This would rule out shear heating as a

cause of melting, a process which we also consider unlikely given the relatively low strain rates ( $10^{11}$ – $10^{13}$  s<sup>-1</sup>) and low differential stresses (tens of MPa) commonly measured in crustal mylonite (Handy and Streit 1999; see also Chapter 6, this volume), and the extreme paucity of shear zones that experienced higher metamorphic temperatures than their enclosing rocks.

Most of the crystallized melt bodies are not concentrated along the STD, but in its footwall (Figures 13.8b, c). This observation is inconsistent with the idea that melts lubricate mylonitic shear zones (Hollister and Crawford 1986; Hodges 1998) in the sense of a pressurized fluid that reduces effective normal stress and resistance to frictional sliding. Where intrusive bodies do occur within the STD, they show various degrees of overprinting, from mylonitic to undeformed (Dèzes et al. 1999). The intrusive bodies never penetrate to the hangingwall of the STD. Some leucogranites that crosscut the STD were thought to intrude its hangingwall (e.g., Guillot et al. 1994; Edwards et al. 1996), but recent work has shown that these granites are deformed by an extensional shear zone of ~300 m width (Searle and Godin 2003) which is not itself intruded by leucogranites and is part of the STD. Mylonitization on subhorizontal shear zones thus acts as a mechanical barrier to the ascent of melt (Handy et al. 2001).

Perhaps the most important feature in the Himalayan sections is the location of most crystallized melt bodies in the central parts of the High Himalayan Crystalline Complex, between the Southern Himalayan detachment system and MCT (Figures 13.8a, b). Based on independent field evidence this area is inferred to represent a former low-viscosity, melt-bearing channel (Grujic et al. 1996) bounded by shear zones with opposite shear senses. We will return to this below in the context of modeling studies.

### *Tertiary Melting and Extension in the North American Cordillera*

Thin, granitic sills have also been found along the mylonitic tops of metamorphic core complexes and they have been inferred to promote localization of deformation (Whipple Mountains, U.S.A.; Lister and Baldwin 1993). Low viscosity bodies must be included in scaled, analogue, and numerical models of metamorphic core complexes in order to obtain localized extension and core complex formation (Brun et al. 1994; Tirel et al. 2004). Thus, melt intrusion may augment localization during extension. In two other metamorphic core complexes of the North American Cordillera, the onset of melting is inferred to precede the onset of extension by a considerable amount of time (10 Ma in the Shuswap core complex, British Columbia, Canada: Vanderhaeghe et al. 1999; 30 Ma in the Bitterroot core complex, Montana, U.S.A.: Foster and Fanning 1997). These authors therefore conclude that melting triggered gravitational collapse by reducing the strength of the lower crust (also Foster et al. 2001).

Yet, these interpretations are partly based on ambiguous, sometimes contradictory data. Decompression of the Shuswap core complex from 10 to 5 kbar

was synchronous with melting (Norlander et al. 2002). However, a temporal distinction between the onset of melting and the onset of extensional faulting is equivocal because both events are dated by the oldest crystallization ages of zircons from synkinematic leucosomes (Vanderhaeghe et al. 1999). In the Bitterroot complex, field evidence points to coeval extensional shearing and magmatism (LaTour and Barnett 1987), but abundant geochronological data indicate prolonged melting and magmatism for at least 30 Ma (beginning before 80 Ma) prior to the onset of extensional deformation at about 53 Ma (Foster and Fanning 1997; Foster et al. 2001). In fact, migmatitic crystallization ages suggest that there were two distinct anatexis events, only the younger of which at ~53 Ma (Foster et al. 2001) was coeval with, or slightly older than the extensional deformation. Thus, gravitational collapse initiated only at the very end of this younger anatexis phase and continued in the absence of magmatism until 43 Ma (Foster and Fanning 1997). If the geochronological data are valid, then anatexis may not have triggered extension, much less the collapse of the Cordilleran orogen. Unfortunately, to our knowledge no structural investigation of the migmatites exists as yet.

The idea that melting triggers syn-orogenic extension is based on the premise that tectonic boundary conditions like the regional convergence rate remained constant for the duration of crustal thickening. This assumption is probably justified for the North American Cordillera, where independent evidence from magnetic anomalies suggests that divergence at the plate boundaries, between the Pacific and the Farallon Plates, began some 10 Ma after the formation of the metamorphic core complexes (Engelbreton et al. 1985; Vanderhaeghe and Teyssier 2001a, b). However, the poor constraints on the large-scale plate kinematics of older orogens such as the Variscides (Malavieille et al. 1990; Ledru et al. 2001; Brown 2005) and Caledonides (White and Hodges 2002; McLelland and Gilotti 2003) may not allow one to distinguish between extension induced by changing boundary conditions and by melt-induced changes in the rheology of the thickened crust. For example, the onset of Early Permian extension and magmatism in the Variscides appears to be related to a switch from head-on collision to dextral transpression between Laurussia and Gondwana (Matte 1991).

## **NUMERICAL MODELING OF FAULTING DURING ANATEXIS**

Numerical models allow one to simulate the flow of melt-bearing layers on the scale of the entire crust and to predict the effects of melting and deformation on the surface features of mountain belts (e.g., Beaumont et al. 2001; Babeyko et al. 2002). At the current state of computing power, the resolution of melt-induced flow is practically limited to the scale size of a numerical cell of several kilometers. This resolution is sufficient to predict large-scale flow patterns, but not suited to investigate the nucleation and propagation of individual

faults. Melting is modeled by assuming that the crust weakens instantaneously upon reaching the solidus, generally taken to be in the range 700–750°C. Therefore, the segregation of melt during deformation, variations in melt pressure, and changes in energy balance associated with melting and crystallization are usually not considered. An exception to this is the study of Babeyko et al. (2002), in which melt segregation is achieved simply by changing the melt volume percent independent of deformation and pressure.

### **Influence of Crustal Melting on the Shape of Orogens**

Bird (1991) predicted that topographic gradients create pressure gradients within the Earth, which induce flow of a weak lower crust and cause topography to flatten. For example, an initially 2 km high and 300 km wide mountain belt can be reduced to 1 km height within tens of millions of years (Bird 1991, Table 2) due to lower-crustal flow, even in the absence of melt. Weakening the lower crust by a factor of 10 to 20 increases the rate of topographic leveling by at least the same order of magnitude, that is, by 10–20 times. The resulting rate of leveling is of the same order of magnitude as the thickening rate of most orogenic systems ( $10^{-3} \text{ m yr}^{-1}$ ). Therefore, orogenesis cannot produce any significant topographic gradients above a partially melted lower crust.

Whereas Bird's model considered local readjustments of topographic gradients, later analytical models investigated the relationship between the shape of

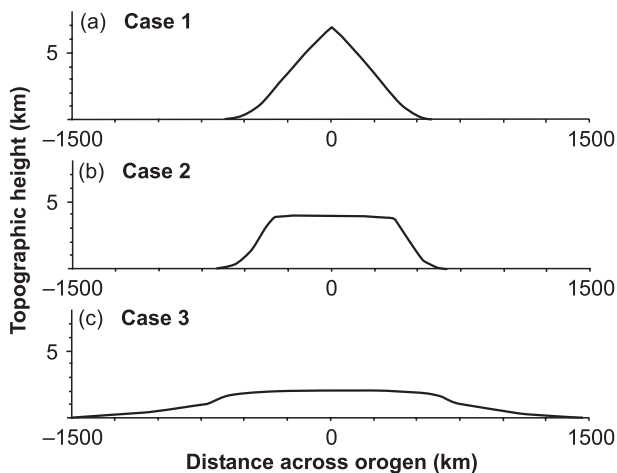


**Figure 13.11** Generic cross-sectional shapes of modeled orogens, from Royden (1996). All cross sections show the orogenic geometry after 16 Ma of shortening. Case 1: Uniform viscosity crust; Case 2: Initial uniform viscosity followed by formation of a low-viscosity zone at the base of the crust; Case 3: Presence of low-viscosity zone at the base of the crust prior to the onset of convergence.

orogens and crustal viscosities (Figure 13.11, Royden 1996). Orogens modeled with uniform crustal rheology acquire triangular cross-sectional shapes (back-to-back wedges in Figure 13.11a), whereas significant weakening of the lower part of the thickened crust results in a plateau-like geometry (Figure 13.11b). Royden (1996) did not explicitly mention melting in the lower crust, but the rheology in her preferred plateau model (Figure 13.11b) is based on a viscosity reduction of almost two orders of magnitude per km depth. Such a drop in viscosity can only occur at the transition from solidus to hypersolidus conditions. Vanderhaeghe et al. (2003) presented a series of models which extended Royden's (1996) model and concluded that partial melting in the orogenic crust can change the shape of an orogen from triangular to plateau-like.

To illustrate the effect of lower crustal melting on the height and the width of a generic orogen, we consider the balance of horizontal forces acting on one half of an evolving orogenic crust subjected to continuous compressional basal traction (Figure 13.12). Our approach follows the models outlined in Medvedev (2002) and Vanderhaeghe et al. (2003). The horizontal compressional force,  $F_c$ , is inversely proportional to the width of the orogen and therefore decreases progressively during growth of the orogen (Medvedev 2002). This force plays a limited role in the balance of forces for a uniformly linear viscous crustal wedge, so we neglect it for the sake of simplicity. The two remaining forces, the gravitational force ( $F_g$ ) associated with a difference in elevation between the mountain range and the foreland and the basal tractional force ( $F_t$ ), must balance:  $F_t = F_g$ . The gravitational force,  $F_g$ , is the difference in potential energy between mountain and foreland.  $F_g$  increases with thickening of the crust. It is proportional to the difference in density between crust and mantle,  $\rho_m - \rho_c$ , and to the square of the change in crustal thickening,  $h_{\max}^2 - h_0^2$ . The basal tractional force,  $F_t$ , is proportional to the viscosity at the base of the crust,  $\eta_c$ , and grows proportionally with the width of the orogen,  $\lambda_c$  (Figure 13.12a). So for a crust with uniform rheology subjected to constant material flux of incoming material, there is no limit to the growth of  $F_t$ , and therefore no limit to the growth of  $F_g$ . Consequently, there is also no limit to the thickness of the orogenic crust,  $h_{\max}$  (Vanderhaeghe et al. 2003).

Melting in the crust changes the force balance significantly (Figure 13.12b). In this case, the base of the crust is characterized by two different viscosities: the viscosity of the solid crust,  $\eta_c$ , and the viscosity of the melt-bearing crust,  $\eta_b \ll \eta_c$ . The basal tractional force,  $F_t$ , becomes the sum of the tractions corresponding to different viscosities:  $F_{tc}$  and  $F_{tb}$ . Assuming that  $F_{tc} \gg F_{tb}$  (because  $\eta_b \ll \eta_c$ ), the force balance in the melt-bearing crust becomes  $F_{tc} = F_g$ . At these conditions the area of the unmelted base of the crust limits the force  $F_{tc}$ , and so  $F_g$  and, consequently also  $h_{\max}$  are limited. Thus, melting at the base of the orogenic crust limits the height of mountains and causes the formation of a plateau. Once established, the plateau widens without significant change in its height (Vanderhaeghe et al. 2003; Beaumont et al. 2004).

The most important assumption made in the derivation above is that  $F_{tc} \gg F_{tb}$ . If partial melting weakens the base of the orogenic crust less significantly (Case 2a in Royden 1996; “double-slope wedge” in Vanderhaeghe

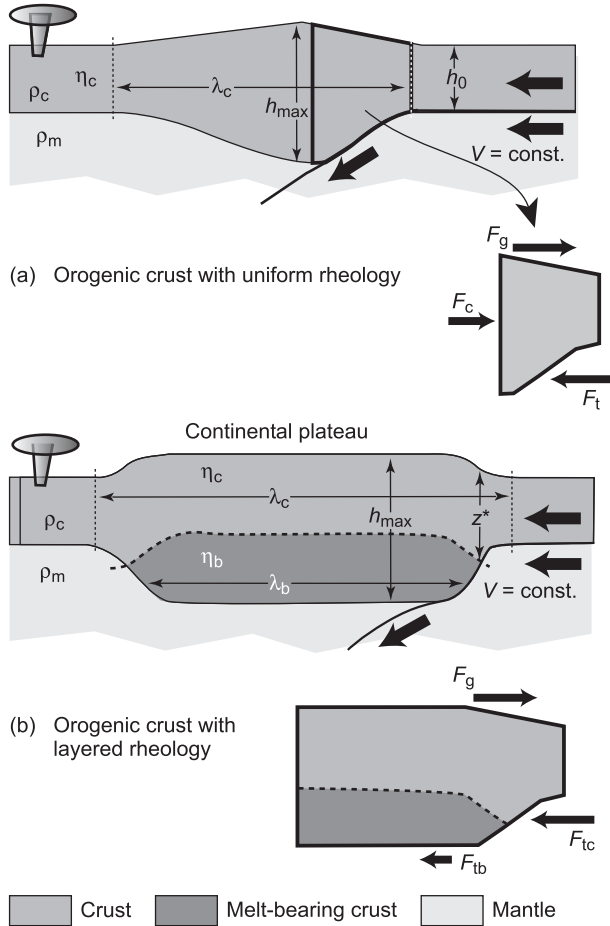


**Figure 13.12** Conceptual model illustrating the deformation style and force balance in orogenic crust. Deformation is driven by convergence at a velocity,  $V$ , and subduction of the mantle lithosphere. The forces stem from gravity,  $F_g$ , compression,  $F_c$ , and traction at the base of the crust,  $F_t$ . (a) Orogenesis with crust of uniform viscosity ( $\eta_c$ ) leads to the formation of “back-to-back wedges” without any limit to the thickness of the crust; (b) Orogenesis with layered crust and rheology leads to the formation of a plateau when  $\eta_c \gg \eta_b$  and  $F_t = 0$ . Basal traction force,  $F_t$ , is divided into two parts reflecting the changes at the base of crust due to the formation of a weak (partially melted) basal layer.  $F_c$  is neglected in the simplified force balance.  $\rho_c$  = density of crust,  $\rho_m$  = density of mantle (modified from Vanderhaeghe et al. 2003).

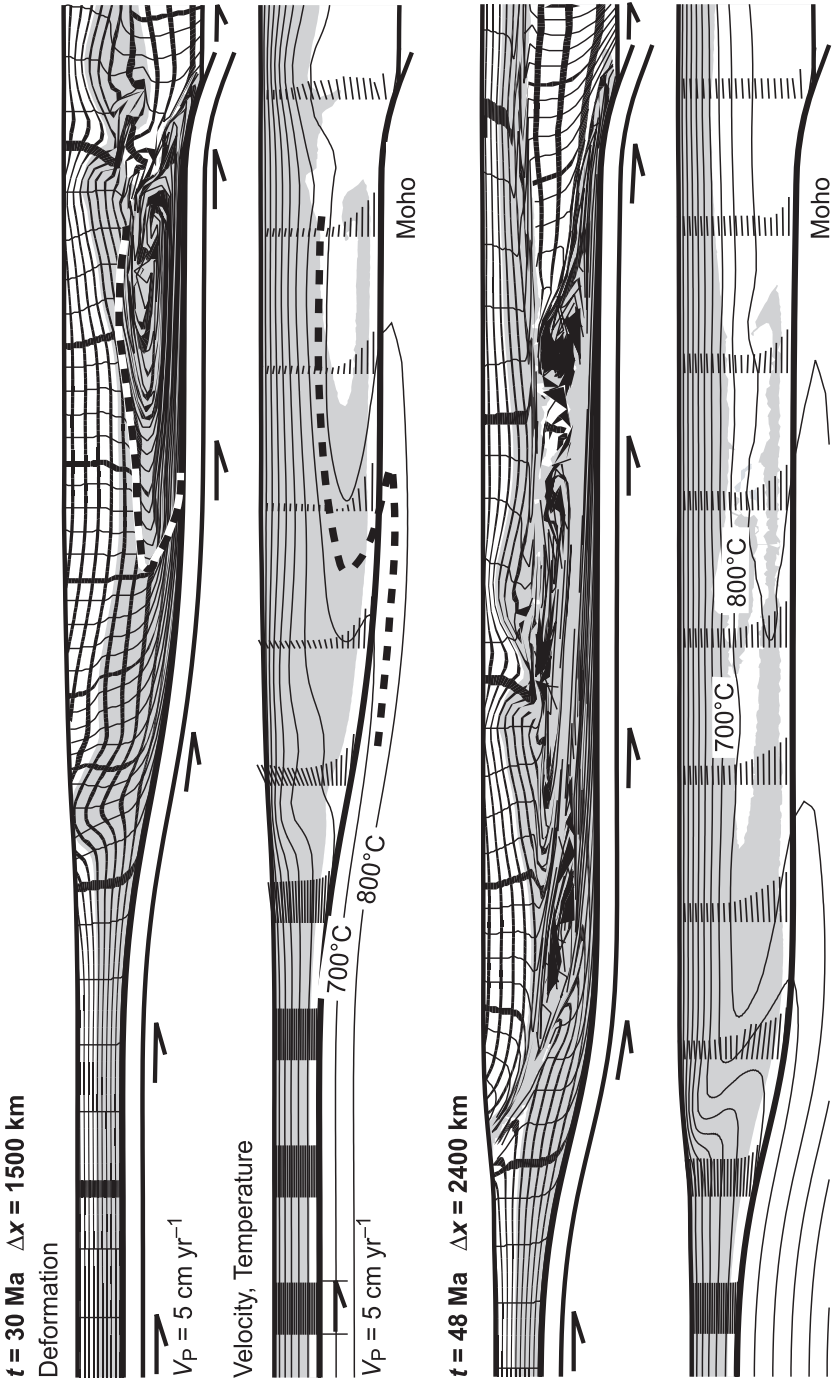
et al. 2003) or if the viscosity of the lower crust decreases monotonously with depth and temperature in the absence of melt-weakening (Model 3 and Figure 6b in Beaumont et al. 2004; Figure 11a in Medvedev and Beaumont 2006), the orogen acquires a shape that is intermediate between wedge-like and plateau-like.

The analysis presented above assumes that the orogenic system is driven at a constant shortening rate by the plate tectonic force, which is theoretically unlimited. However, translation of this force into orogenic deformation is limited by the rheological properties of the crust, hence by melting. A similar conclusion is reached by considering that the compressive forces involved during orogenesis are not unlimited, preventing lithospheric thickening and mountain chains from growing beyond a given height (Molnar and Lyon-Caen 1988, p. 195). The model presented above differs in that it is based on the analysis of viscosity changes due to melting of the crust. These changes are better constrained than the forces driving orogenesis.

### **Case Studies of Deformation in the Presence of Partially Melted Mid- to Lower Crust**

Beaumont and colleagues (Beaumont et al. 2001, 2004; Jamieson et al. 2002, 2004; Vanderhaeghe et al. 2003) developed thermomechanical models in which the effective viscosity of the lower crust is reduced during shortening in order to simulate a melt-bearing crustal layer below Tibet (e.g., Nelson et al. 1996). If viscosity is reduced to  $10^{19}$  Pa s or less at temperatures of 700–750°C, then the weakened part of the lower crust flows laterally within a channel (Figure 13.13). This melt-induced viscosity reduction is actually not very great: only an order of magnitude less than the adjacent, unmelted rock. However, it is important to point out that greater viscosity reductions (to  $10^{18}$  Pa s or less) do not significantly change the result—orogens underlain by enough melt to weaken the crust by at least an order of magnitude always develop plateaus (Beaumont et al. 2001; Vanderhaeghe et al. 2003). We note that these values of viscosity are in line with the theoretically derived flow laws for granitoid rocks of intermediate grain size and composition, containing 2 to 5 vol.-% of melt (Figure 13.4). Models without a low-viscosity layer (i.e., melt-absent) show little if any lower crustal flow and no pronounced development of a plateau-like topography (Beaumont et al. 2004, their Model 3). The melt-bearing layer and crustal channel coincide exactly in all models. In other words, the lateral extent of channel flow always matches the increase in lateral extent of the melt-bearing layer (Figure 13.13a; Beaumont et al. 2004, their Figures 3 and 10). Melting in the lower crust results in instantaneous lateral propagation of the melted domain within a channel.

Models incorporating channel flow successfully explain the formation of the first-order structure of the Himalayan-Tibetan system (Beaumont et al. 2001,



2004) and the exhumation of Miocene migmatitic rocks from beneath the Tibetan Plateau (e.g., Grujic et al. 1996; Jamieson et al. 2004) in response to topographic loading and enhanced erosion (e.g., Wu et al. 1998). If the top of the melt-bearing channel in the model of Beaumont et al. (2004) is taken to represent the STD (Figure 13.8a), then the anatectic rocks of the High Himalayan Crystalline Complex represent the flowing channel of melt-bearing rocks whose movement coincided with the onset of extension along the STD.

We note that modeled and natural orogenic cross sections are only similar if the erosion rate at the southern boundary of the plateau is assumed to be extremely high ( $1 \text{ cm yr}^{-1}$ ). If not, then the low-viscosity channel is not drawn to the surface, and anatectic rocks are not exhumed. Only the highest reported erosion rates in the Himalayas are comparable to this value ( $2\text{--}12 \text{ mm yr}^{-1}$ ; Burbank et al. 1996) which are themselves greater than in the central Andes (e.g., Montgomery et al. 2001). This may explain why, although both plateaus are inferred to overlie a melt-bearing crustal layer, no extrusion and exhumation of this layer takes place in the Andes. Comparison of long-term erosion rates in both Tibet and the Andes (methods described in Chapter 9) could constrain the effect of erosion on the geometry of faults in orogens that overlie melt-bearing crust.

Babeyko et al. (2002) demonstrate a different effect of partial melting at the base of the Andean Plateau in their thermomechanical model of the Andean subduction orogen. Petrological data indicate that the orogenic crust in this region became extremely hot ( $800^\circ\text{C}$ , at 20 km depth) during the formation and evolution of the plateau (20 Ma). To match these data,

- 
- ◀ **Figure 13.13** Two stages of convergence modeled for a region corresponding to the Himalayas and southern Tibet (from Beaumont et al. 2004). Half arrows indicate the movement of the subducting (Indian) lower plate lithosphere. Deformation of the finite element grid outlines the site of the partially melted, midcrustal channel. For details on thermomechanical parameters, see Beaumont et al. (2004). (a) After 1500 km of shortening: The  $750^\circ\text{C}$  isotherm (stippled line interpolated between  $700^\circ\text{C}$  and  $800^\circ\text{C}$  isotherms) is a proxy for the melt front and outlines the partially melted area in the crust. The site and shape of this isotherm closely matches the margin of the channel as defined by the deformed finite element grid. The coincidence of the melting front and the channel front suggests a nearly instantaneous propagation of channel flow into the newly melted midcrust. This feature can be observed at all stages of the model (Beaumont et al. 2004). An antiformal structure has formed at the margin of the plateau and is caused by localized erosion. (b) After 2400 km of shortening. Lateral propagation of the melt-bearing channel leads to formation of the antiformal structure at the erosional front. Note the upper-crustal antiformal structures, whose position is similar to the gneiss domes north of the STD in Figure 13.8a.

Babeyko et al. (2002) introduced a very high mantle heat flow at the base of the model ( $60 \text{ mW m}^{-2}$ ), which leads to melting of the lower crust, melt segregation, and a reduction of lower-crustal viscosity to  $10^{17} \text{ Pa s}$ . This value is consistent with a melt content of about 20 vol.-% estimated from geoelectric measurements (Schilling and Partzsch 2001) and leads to convection of the lower Andean crust (Babeyko et al. 2002). Models in which crustal convection was inhibited and/or in which the basal heat flow was less than  $60 \text{ mW m}^{-2}$  failed to match the petrological interpretations ( $800^\circ\text{C}$  at 20 km depth after 20 Ma of orogenesis).

### **Interaction of Crustal Melts with Brittle Upper Crust**

The effect of lower-crustal channel flow on the brittle upper crust was investigated in a series of numerical experiments in which the crust is weakened by a combination of rapid denudation along the plateau flank and thermal weakening due to heat advected by the channel (Figure 13.13; Beaumont et al. 2001, 2004). The upper crust becomes unstable and slides laterally under the force of gravity. This lateral migration involves thrusting at the plateau margin and normal faulting within the plateau. The low-viscosity (melt-bearing) material flows into the extensional area within the plateau, forming gneiss domes analogous to those exposed north of the STD (GD in Figure 13.8a; Figure 13.13b; Lee et al. 2000). Note that this extensional feature was modeled in the plane containing the direction of convergence between India and Asia. However, similar translation of the upper crust above the weak, lower crust can also effect out-of-section motion, for example, eastward lateral extrusion of Tibet (e.g., Medvedev and Beaumont 2006), as inferred from east–west directed rifting in Southern Tibet (Masek et al. 1994).

In their model of the Altiplano plateau in the Andes, Babeyko et al. (2002) also predicted pronounced faulting of the upper crust above a melt-weakened lower crust during shortening (their Figure 7). However, detailed investigation of the relationship between melting and crustal-scale faulting is limited by the low spatial resolution of the numerical model.

Analytical models provide an alternative approach to investigate the effects of melting on the deformation of the brittle part of the crust. Though based on simple assumptions, analytical models are independent of a given spatial resolution and hence very useful for investigating specific interaction of melts and faults. However, these simplifications may lead to incorrect results. For example, some analytical models employ a purely elastic rheology to approximate the distribution of stresses in the brittle crust (Parsons and Thompson 1993), and predict that extensional faults nucleated near dykes have a low-angle geometry. However, the use of a fully numerical approach and theoretical analysis showed that the latter orientation results from the unrealistic rheology of the boundary conditions (Gerbault et al. 1998).

## CONCLUSIONS AND FUTURE OUTLOOK

A small amount of melt has a great effect on the geometry of mountain belts, faults, and shear zones. Melt-bearing crustal rocks deformed at different experimental conditions all show an exponential decay of strength with increasing melt percentage. The greatest strength drop, of about one order of magnitude, takes place between the onset of melting and  $\sim 7$  vol.-% melt (Figure 13.2). Experimental results on melt-bearing olivine aggregates, and theoretically derived flow laws for melt-bearing granite show that the viscosity decreases most strongly at very low melt volumes (3 to 5%; Figures 13.5 and 13.6), whereas for melt volumes  $>5\%$  the decrease in viscosity is much less pronounced (Figures 13.5 and 13.6). Several observations from natural and modeling studies suggest that the attainment of this transition is associated with a first-order change in the tectonic and topographic style of orogens. As shown for the Indian–Asian collision, a plateau formed above crust inferred to contain 5–14 vol.-% melt, but not where melt volume is inferred to be 4% (Unsworth et al. 2005). In addition, geodynamic modeling shows that the onset of plateau formation and channel flow in the lower crust is triggered by a melt-induced viscosity reduction of one order of magnitude in the lower crust, i.e., the viscosity reduction corresponding to  $\sim 5$  vol.-% of melt (Figures 13.5 and 13.6). Modeling also shows that any additional weakening of the lower crust does not significantly change the tectonic style (Beaumont et al. 2001).

The structural and mechanical causes underlying this strength drop have yet to be investigated thoroughly. We suspect that it is controlled by the degree of melt connectivity, in that increasing melt interconnectivity induces grain-boundary sliding and thereby enhances granular flow (Hirth and Kohlstedt 1995a, b; Rosenberg and Handy 2005). To test this hypothesis on crustal rocks, deformation experiments should be combined with detailed microstructural investigation of the evolving 3D melt network at the grain boundaries, especially at melt volumes less than 10%. In addition, new experiments are needed to establish whether mechanical steady state can be achieved for melt-assisted viscous granular flow, and hence derive a constitutive flow law. Determining whether or not the same grain-scale mechanisms operate in the laboratory specimens as in naturally deformed rocks would be an important first step toward establishing at least a phenomenological basis for extrapolating flow laws for melt-bearing rocks.

Large bodies of melt can reside in the crust for up to 20 Ma, possibly longer. Because they localize strain so effectively, such bodies can spread laterally to form weak, subhorizontal channels which drive the lateral topographic growth of the orogen. In fact, numerical modeling suggests that partially melted channels are a requisite for the growth of orogenic plateaus like those presently observed in the central Andes and Tibet. Melt thus plays a major role in shaping orogens. Despite general agreement that melt drastically weakens the crust and fosters vertical decoupling, there is still no consensus on whether melting

can trigger gravitational collapse of thickened crust, and if so, what amount of melt is necessary to induce such a large-scale process.

The latter point has rarely been addressed in field investigations. Ideally, future studies would focus on the relationship of strain gradients to gradients in crystallized melt content to evaluate the influence of melt on structural style. Yet, correlating structural style with melt content in natural exposures of anatectic rock is very difficult, if not impossible, for the following reasons: (a) leucosomes taken to represent the melt are generally cumulate or fractionated liquids (Solar and Brown 2001); (b) leucosomes may only represent the small amount of melt remaining at crystallization, rather than the greater volume which originally resided in the rock prior to crystallization; (c) deformation often severely modifies or overprints structures associated with melt and melting.

Establishing whether or not melting triggers gravitational collapse, requires evidence that the onset of melting preceded the onset of crustal extension over the entire area affected by extension. This requires radiometric ages of igneous minerals that grew in the syntectonic melt as well as formational ages of metamorphic minerals that form the dominant schistosity in the extensional shear zones. No studies so far provide such independent ages, relying instead on one or the other (melt and shear zone) ages to date both events.

In the case of a Himalayan-Tibetan-type orogen with a melt-weakened intracrustal channel, numerical modeling (Beaumont et al. 2001) indicates that melting (inferred to attain ~5%) should be nearly contemporaneous with the formation and lateral propagation of the channel and the extrusional flow of melt-bearing rock within it. The subhorizontal channel is bounded along its base and roof by large shear zones with opposite shear senses. At the orogenic scale, these shear zones are recognized as low-angle thrusts and normal faults that accommodate the extrusion of partially melted crust in between. The MCT and the Southern Tibetan detachment system in the Himalayas exemplify such an extrusional system. Together with their bounding shear zones, the channels form a new class of fault which we term "extrusional faults." Exhumation due to extrusional flow is very different from extensional exhumation of anatectic rocks in the footwall of low-angle extensional detachments in the North American Cordillera. However, it is kinematically related to the buoyancy-driven, return motion of subducted crustal slivers that detach from the down-going lithospheric slab, as modeled by Chemenda et al. (1995). Like the extruded anatectites in the Himalayas, these exhuming coherent slivers are bounded above and below by normal faults and thrusts, respectively.

Strike-slip and oblique-slip faults are effective pathways for the rapid, buoyant rise of melts through the crust. These faults may or may not nucleate during melting. The relatively short residence time of melts in these fault systems (<1–2 Ma) can lead to episodic motion, with long periods of creep punctuated by shorter periods of melt veining, magmatic activity and/or faster slip (Handy et al. 2001).

Continental crust subjected to very high heat flux from the asthenosphere may attain melt volumes in excess of the critical 5–7 vol.-% required for localization and decoupling. If the melt content reaches 20–25 vol.-% under these conditions, then crustal shortening can trigger convective overturn of the melt-bearing crust (Babeyko et al. 2002). However, this process, which was proposed to explain “dome and keel” structures of the Archaean crust (Collins et al. 1998), is not yet supported by field studies on Phanerozoic orogens.

Geodynamic models that include the effect of melting on deformation are in their infancy. These models are only valid for 2D plane strain deformation, whereas the interaction between melts and oblique-slip faults is a 3D problem awaiting further investigation. The challenge in using these sophisticated models will be to treat them as controlled experiments and parameter studies rather than as simulations with a large number of interactive, yet poorly constrained variables.

### ACKNOWLEDGEMENTS

Discussions with Ulrich Riller and constructive reviews by Mike Brown and Greg Hirth significantly improved our manuscript. Martyn Unsworth kindly provided a preprint of his work. We acknowledge the support of the German Science Foundation (DFG) in the form of grants RO 2177/1-1, HA 2403/3-1, HA 2403/6-1, and project G2 of the SFB-267 “Deformation Processes in the Andes,” which provided funding for parts of our work.

### REFERENCES

- Armstrong, R.L., and P. Ward. 1991. Evolving geographic patterns of Cenozoic magmatism in the Northern American Cordillera: The temporal and spatial association of magmatism and metamorphic core complexes. *J. Geophys. Res.* **96**:13,201–13,224.
- Arzi, A. 1978. Critical phenomena in the rheology of partially melted rocks. *Tectonophysics* **44**:173–184.
- Babeyko, A.Y., S.V. Sobolev, R.B. Trumbull, O. Oncken, and L.L. Lavie. 2002. Numerical models of crustal scale convection and partial melting beneath the Altiplano-Puna Plateau. *Earth Planet. Sci. Lett.* **199**:373–388.
- Beaumont, C., P. Fullsack, and J. Hamilton. 1994. Styles of crustal deformation in compressional orogens caused by subduction of the underlying lithosphere. *Tectonophysics* **232**:119–132.
- Beaumont, C., R.A. Jamieson, M.H. Nguyen, and B. Lee. 2001. Himalayan tectonics explained by extrusion of a low-viscosity channel coupled to focused surface denudation. *Nature* **414**:738–742.
- Beaumont, C., R.A. Jamieson, M.H. Nguyen, and S. Medvedev. 2004. Crustal channel flows: 1. Numerical models with applications to the tectonics of the Himalayan-Tibetan orogen. *J. Geophys. Res.* **109**:B06406, doi:10.1029/2003JB002809.
- Berger, A., C.L. Rosenberg, and S.M. Schmid. 1996. Ascent, emplacement and exhumation of the Bergell pluton within the Southern Steep Belt of the Central Alps. *Schweiz. Mineral. Petrograph. Mitt.* **76**:357–382.

- Biddle, K.T., and N. Christie-Blick. 1985. Strike-slip deformation, basin formation, and sedimentation, Spec. Publ. 37, pp. 127–142. Tulsa, OK: Soc. Econ. Paleontologists and Mineralogists.
- Bird, P. 1991. Lateral extrusion of lower crust from under high topography, in the isostatic limit. *J. Geophys. Res.* **96**:10,275–10,286, 10.1029/91JB00370.
- Brown, M. 2005. Synergistic effects of melting and deformation: An example from the Variscan belt, western France. In: *Deformation Mechanisms, Rheology and Tectonics: From Minerals to the Lithosphere*, ed. D. Gapais, J.P. Brun, and P.R. Cobbold, Spec. Publ. 243, pp. 205–225. London: Geol. Soc.
- Brown, M., and R.D. Dallmeyer. 1996. Rapid Variscan exhumation and role of magma in core complex formation: Southern Brittany metamorphic belt, France. *J. Metamorphic Geol.* **14**:361–379.
- Brown, M., and T. Rushmer. 1997. The role of deformation in the movement of granitic melt: Views from the laboratory and the field. In: *Deformation-enhanced Fluid Transport in the Earth's Crust and Mantle*, ed. M.B. Holness, Mineral. Soc. Ser. 8, pp. 111–144. London: Chapman and Hall.
- Brown, M., and G.S. Solar. 1998. Shear zone systems and melts: Feedback relations and self-organization in orogenic belts. *J. Struct. Geol.* **20**:211–227.
- Brown, M., and G.S. Solar. 1999. The mechanism of ascent and emplacement of granite magma during transpression: A syntectonic granite paradigm. *Tectonophysics* **312**:1–33.
- Brown, R.L., and J.H. Nazarchuk. 1993. Annapurna detachment fault in the Greater Himalaya of central Nepal. In: *Himalayan Tectonics*, ed. P.J. Treloar, and M.P. Searle, Spec. Publ. 74, pp. 461–473. London: Geol. Soc.
- Bruhn, D., N. Groebner, and D.L. Kohlstedt. 2000. An interconnected network of core-forming melts produced by shear deformation. *Nature* **403**:883–886.
- Brun, J.-P. 1999. Narrow rifts versus wide rifts: Inferences for the mechanics of rifting from laboratory experiments. *Phil. Trans. R. Soc. Lond. A* **357**:695–712.
- Brun, J.-P., D. Sokoutis, and J. Van Den Driesche. 1994. Analogue modelling of detachment fault systems. *Geology* **22**:319–322.
- Burbank, D.W., J. Leland†, E. Fielding et al. 1996. Bedrock incision, rock uplift and threshold hillslopes in the northwestern Himalayas. *Nature* **379**:505–510
- Burchfiel, B.C., Z. Chen, K.V. Hodges et al. 1992. The South Tibetan Detachment System, Himalayan Orogen: Extension Contemporaneous with and Parallel to Shortening in a Collisional Mountain Belt, Spec. Paper 269, p. 41. Boulder, CO: Geol. Soc. Am.
- Chemenda, A.I., M. Mattauer, J. Malavieille, and A.N. Bokum. 1995. A mechanism for syn-collisional rock exhumation and associated normal faulting: Results from physical modeling. *Earth Planet. Sci. Lett.* **132**:225–232.
- Collins, W.J., M.J. van Kranendock, and C. Teyssier. 1998. Partial convective overturn of Archaean crust in the eastern Pilbara Craton, Western Australia: Driving mechanisms and tectonic implications. *J. Struct. Geol.* **20**:1405–1424.
- Coney, P.J., and T.A. Harms. 1984. Cordilleran metamorphic core complexes: Cenozoic extensional relics of Mesozoic compression. *Geology* **12**:550–554.
- Cruden, A.R. 1990. Flow and fabric development during the diapiric rise of magma. *J. Geol.* **98**:681–698.
- Davidson, C., L.S. Hollister, and S.M. Schmid. 1992. Role of melt in the formation of a deep-crustal compressive shear zone: The MacLaren glacier metamorphic belt, South Central Alaska. *Tectonics* **11**:348–359.

- de Saint-Blanquat, M., B. Tikoff, C. Teyssier, and J.L. Vigneresse. 1998. Transpressional kinematics and magmatic arcs. In: *Continental Transpressional and Transensional Tectonics*, ed. R.E. Holdsworth, R.A. Strachan, and J.F. Dewey, Spec. Publ. 135, pp. 327–340. London: Geol. Soc.
- de Silva, S.L. 1989. Geochronology and stratigraphy of the ignimbrites from the 21°30' S portion of the Central Andes of N. Chile. *J. Volcanol. & Geotherm. Res.* **37**:93–131.
- Dell'Angelo, L.N., and J. Tullis. 1988. Experimental deformation of partially melted granitic aggregates. *J. Metamorphic Geol.* **6**:495–515
- Dèzes, P.J., J.-C. Vannay, A. Steck, F. Bussy, and M. Cosca. 1999. Synorogenic extension: Quantitative constraints on the age and displacement of the Zaskar shear zone (northwest Himalaya). *Bull. Geol. Soc. Am.* **111**:364–374.
- D'Lemos, R.S., M. Brown, and R.A. Strachan. 1992. Granite magma generation, ascent and emplacement within a transpressional orogen. *J. Geol. Soc. Lond.* **149**:487–490.
- Edwards, M.A., W.S.F. Kidd, J. Li, Y. Yue, and M. Clark. 1996. Multi-stage development of the southern Tibet detachment system near Khula Kangri. New data from Gonto La. *Tectonophysics* **260**:1–19.
- Edwards, M.A., and M.T. Harrison. 1997. When did the roof collapse? Late Miocene north–south extension in the high Himalaya revealed by Th-Pb monazite dating of the Khula Kangri granite. *Geology* **25**:543–546.
- Engelbreton, D.C., A. Cox, and R.G. Gordon. 1985. Relative Motions between Oceanic and Continental Plates in the Pacific Basin, Spec. Paper 206. Boulder, CO: Geol. Soc. Am.
- England, P., P. Le Fort, P. Molnar, and A. Pecher. 1992. Heat sources for Tertiary metamorphism and anatexis in the Annapurna Manaslu region of Central Nepal. *J. Geophys. Res.* **97**:2107–2128.
- Fitch, T.J. 1972. Plate convergence, transcurrent faults, and internal deformation adjacent to southeast Asia and the Western Pacific. *J. Geophys. Res.* **77**:4432–4460.
- Foster, D.A., and C.M. Fanning. 1997. Geochronology of the northern Idaho batholith and the Bitterroot metamorphic core complex: Magmatism preceding and contemporaneous with extension. *Bull. Geol. Soc. Am.* **109**:379–394.
- Foster, D.A., C. Schafer, C.M. Fanning, and D.W. Hyndmann. 2001. Relationships between crustal partial melting, plutonism, orogeny, and exhumation: Idaho-Bitterroot batholith. *Tectonophysics* **342**:313–350.
- Froitzheim, N., S.M. Schmid, and M. Frey. 1996. Mesozoic paleogeography and the timing of eclogite-facies metamorphism in the Alps: A working hypothesis. *Eclogae Geologicae Helveticae* **89**:81–110.
- Gaillard, F., B. Scaillet, and M. Pichavant. 2004. Evidence for present-day leucogranite pluton growth in Tibet. *Geology* **32**:801–804, doi:10.1130/G20577.1
- Gerbault, M., A.N.B. Poliakov, and M. Daignieres. 1998. Prediction of faulting from theories of elasticity and plasticity: What are the limits? *J. Struct. Geol.* **20**: 301–320.
- Glazner, A.F. 1991. Plutonism, oblique subduction, and continental growth: An example from the Mesozoic of California. *Geology* **19**:784–786.
- Gleason, G.C., and J. Tullis. 1995. A flow law for dislocation creep of quartz aggregates determined with the molten salt cell. *Tectonophysics* **247**:1–23.
- Grujic, D., M. Casey, C. Davidson et al. 1996. Ductile extrusion of the Higher Himalayan Crystalline in Bhutan: Evidence from quartz microfabrics. *Tectonophysics* **260**:21–44.

- Guillot, S., K. Hodges, P. Le Fort, and A. Pecher. 1994. New constraints on the age of the Manaslu granite: Evidence for episodic tectonic denudation in the Central Himalayas. *Geology* **22**:559–562.
- Günther, A. 2001. Strukturgeometrie, Kinematik und Deformationsgeschichte des oberkretazisch-alttertiären magmatischen Bogens (Nord-chilenische Präkordillere 21.7–23°S). Ph.D. diss., Freie Universität Berlin, p. 170.
- Handy, M.R., A. Mulch, M. Rosenau, and C.L. Rosenberg. 2001. A synthesis of the role of fault zones and melts as agents of weakening, hardening and differentiation of the continental crust. In: *The Nature and Tectonic Significance of Fault Zone Weakening*, ed. R.E. Holdsworth et al., Spec. Publ. 186, pp. 305–332. London: Geol. Soc.
- Harris, N., and J. Massey. 1994. Decompression and anatexis of Himalayan metapelites. *Tectonophysics* **13**:1537–1546.
- Harris, N.B.W., M. Caddick, J. Kosler et al. 2004. The pressure-temperature-time path of migmatites from the Sikkim Himalaya. *J. Metamorphic Geol.* **22**:249–264.
- Harrison, M.T., M. Grove, K.D. McKeegan et al. 1999. Origin and episodic emplacement of the Manaslu Intrusive Complex, Central Himalaya. *J. Petrol.* **40**:3–19.
- Hirth, G., J. Escartin, and J. Lin. 1998. The rheology of the lower oceanic crust: Implications for lithospheric deformation at mid-ocean ridges. In: *Faulting and Magmatism at Mid-Ocean Ridges*, ed. W. Buck, P. Delaney, J. Karson, and Y. Lagabriele, Geophys. Monogr. 106, pp. 291–303. Washington, D.C.: Am. Geophys. Union.
- Hirth, G., and D.L. Kohlstedt. 1995a. Experimental constraints on the dynamics of the partially molten upper mantle: Deformation in the diffusion creep regime. *J. Geophys. Res.* **100**:1981–2001.
- Hirth, G., and D.L. Kohlstedt. 1995b. Experimental constraints on the dynamics of the partially molten upper mantle. 2. Deformation in the dislocation creep regime. *J. Geophys. Res.* **100**:15,441–15,449.
- Hirth, G., and D.L. Kohlstedt. 1996. Water in the oceanic upper mantle: Implications for rheology, melt extraction and the evolution of the lithosphere. *Earth Planet. Sci. Lett.* **144**:93–108.
- Hirth, G., and D. Kohlstedt. 2003. Rheology of the upper mantle and the mantle wedge: A view from the experimentalists. In: *Inside the Subduction Factory*, ed. J. Eiler, Geophys. Monogr. 103, pp. 83–105. Washington, D.C.: Am. Geophys. Union.
- Hodges, K.V. 1998. The thermodynamics of Himalayan orogenesis. In: *What Drives Metamorphism and Metamorphic Reactions?* ed. P.J. Treloar and P.J. O'Brien, Spec. Publ. 138, pp. 7–22. London: Geol. Soc.
- Hodges, K.V., R.R. Parrish, and M.P. Searle. 1996. Tectonic evolution of the central Annapurna Range, Nepalese Himalayas. *Tectonics* **15**:1264–1291.
- Hollister, L.S. 1993. The role of melt in the uplift and exhumation of orogenic belts. *Chem. Geol.* **108**:31–48.
- Hollister, L.S., and M.L. Crawford. 1986. Melt-enhanced deformation: A major tectonic process. *Geology* **14**:558–561.
- Holyoke, III, C.W., and T. Rushmer. 2002. An experimental study of grain-scale melt segregation mechanisms in two common crustal rock types. *J. Metamorphic Geol.* **20**:493–512.
- Hopper, J.R., and R.W. Buck. 1998. Styles of extensional decoupling. *Geology* **26**:699–702.
- Houseman, G.A., D.P. McKenzie, and P. Molnar. 1981. Convective instability of a thickened boundary layer and its relevance for the thermal evolution of continental convergent belts. *J. Geophys. Res.* **86**:B7, 6115–6132.

- Huerta, A.D., L.H. Royden, and K.V. Hodges. 1996. The interdependence of deformational and thermal processes in mountain belts. *Science* **273**:637–639.
- Ingram, G.M., and D.H.W. Hutton. 1994. The Great Tonalite Sill: Emplacement into a contractional shear zone and implications for Late Cretaceous to early Eocene tectonics in southeastern Alaska and British Columbia. *Bull. Geol. Soc. Am.* **106**: 715–728.
- Jamieson, R.A., C. Beaumont, S. Medvedev, and M.H. Nguyen. 2004. Crustal channel flows: 2. Numerical models with implications for metamorphism in the Himalayan-Tibetan Orogen. *J. Geophys. Res.* **109**:B06407, doi:10.1029/2003JB002811.
- Jamieson, R.A., C. Beaumont, M.H. Nguyen, and B. Lee. 2002. Interaction of metamorphism, deformation and exhumation, in large hot orogens. *J. Metamorphic Geol.* **20**:9–24.
- Jarrard, R.D. 1986. Relations among subduction parameters. *Rev. Geophys.* **24**:217–284.
- Karato, S. 1986. Does partial melting reduce the creep strength of the upper mantle? *Nature* **319**, 309–310.
- Kohn, M.J., M.S. Wieland, C.D. Parkinson, and B.N. Upreti. 2005. Five generations of monazite in Langtang gneisses: Implications for chronology of the Himalayan metamorphic core. *J. Metamorphic Geol.* **23**:399–406. doi:10.1111/j.1525-1314.2005.00584.x
- Koons, P.O., R.J. Norris, D. Craw, and A.F. Cooper. 2003. Influence of exhumation on the structural evolution of transpressional plate boundaries: An example from the Southern Alps, New Zealand. *Geology* **31**:3–6.
- Lamb, S., L. Hoke, L. Kennan, and J. Dewey. 1997. Cenozoic evolution of the Central Andes in Bolivia and northern Chile. In: *Orogeny through time*, ed. J.P. Burg, and M. Ford, Spec. Publ. 121, pp. 237–264. London: Geol. Soc.
- LaTour, T.E., and R.L. Barnett. 1987. Mineralogical changes accompanying mylonitization in the Bitterroot dome of the Idaho batholith: Implications for timing of deformation. *Bull. Geol. Soc. Am.* **98**:356–373.
- Ledru, P., G. Courrioux, C. Dallain et al. 2001. The Velay dome (French Massif Central): Melt generation and granite emplacement during orogenic evolution. *Tectonophysics* **342**:207–237.
- Lee, J., B.R. Hacker, W.S. Dinklage et al. 2000. Evolution of the Kangmar Dome, southern Tibet: Structural, petrologic, and thermochronologic constraints. *Tectonics* **19**:872–895. doi:1999TC001147.
- Le Fort, P. 1975. Himalayas: The collided range. Present knowledge of the continental arc. *Am. J. Sci.* **275A**:1–44.
- Lejeune, A. and P. Richet. 1995. Rheology of crystal-bearing silicate melts: An experimental study at high viscosities. *J. Geophys. Res.* **100**:4215–4229.
- Li, S., M.J. Unsworth, J.R. Booker, W. Wei, H. Tan, and A.G. Jones. 2003. Partial melt or aqueous fluids in the Tibetan crust: Constraints from INDEPTH magnetotelluric data. *Geophys. J. Intl.* **153**:289–304.
- Lister, G.S., and S.L. Baldwin. 1993. Plutonism and the origin of metamorphic core complexes. *Geology* **21**:607–610.
- Malavieille, J., P. Guihot, S. Costa, J.M. Lardeaux, and V. Gardien. 1990. Collapse of thickened Variscan crust in the French Massif Central: Mont Pilat extensional shear zone and St. Etienne upper Carboniferous basin. *Tectonophysics* **177**:139–149.
- Marchildon, N., and M. Brown. 2002. Grain-scale melt distribution in two contact aureole rocks: Implication for controls on melt localization and deformation. *J. Metamorphic Geol.* **20**:381–396.

- Masek, J.G., B.L. Isacks, E.J. Fielding, and J. Browaeys. 1994. Rift flank uplift in Tibet: Evidence for a viscous lower crust. *Tectonics* **13**:659–667.
- Matte, P. 1991. Accretionary history and crustal evolution of the Variscan belt in western Europe. *Tectonophysics* **196**:309–337.
- McCaffrey, K. 1992. Igneous emplacement in a transpressive shear zone: Ox Mountains igneous complex. *J. Geol. Soc. Lond.* **149**:221–235.
- McClelland, W.C., and J.A. Gilotti. 2003. Late-stage extensional exhumation of high-pressure granulites in the Greenland Caledonides. *Geology* **31**:259–262.
- McNulty, B.A., D.L. Farber, G.S. Wallace, R. Lopez, and O. Palacios. 1998. Role of plate kinematics and plate-slip-vector partitioning in continental magmatic arcs: Evidence from the Cordillera Blanca, Peru. *Geology* **26**:827–830.
- Mechie, J., S.V. Sobolev, L. Ratschbacher et al. 2004. Precise temperature estimation in the Tibetan crust from seismic detection of the  $\alpha$ - $\beta$  quartz transition. *Geology* **32**:601–604.
- Medvedev, S. 2002. Mechanics of viscous wedges: Modeling by analytical and numerical approaches. *J. Geophys. Res.* **107**, 10.1029/2001JB000145
- Medvedev, S., and C. Beaumont. 2006. Growth of continental plateaus by channel injection: Constraints and thermo-mechanical consistency. In: Channel Flow, Ductile Extrusion and Exhumation in Continental Collision, ed. R.D. Law, M.P. Searle, and L. Godin, Spec. Publ. London: Geol. Soc., in press.
- Milliman, J.D., and J.P.M. Syvitski. 1992. Geomorphic/tectonic control of sediment discharge to the ocean: The importance of small mountainous rivers. *J. Geol.* **100**:525–544.
- Molnar, P., and Lyon-Caen, H. 1988. Some Simple Physical Aspects of the Support, Structure, and Evolution of Mountain Belts, Spec. Paper 218, pp. 179–207. Boulder, CO: Geol. Soc. Am.
- Montgomery, D.R., G. Balco, and S.D. Willett. 2001. Climate, tectonics, and the morphology of the Andes. *Geology* **29**:579–582.
- Nelson, K.D., W. Zhao, L.D. Brown et al. 1996. Partially molten middle crust beneath southern Tibet: Synthesis of Project INDEPTH results. *Science* **274**:1684–1687
- Neves, S.P., A. Vauchez, and C.J. Archanjo. 1996. Shear zone-controlled magma emplacement or magma-assisted nucleation of shear zones? Insights from northeast Brazil. *Tectonophysics* **262**:349–364.
- Norlander, B.N., D.L. Whitney, C. Teyssier, and O. Vanderhaeghe. 2002. Partial melting and decompression of the Thor-Odin Dome, Shuswap metamorphic core complex, Canadian Cordillera. *Contrib. Mineral. & Petrol.* **61**:103–125.
- Oberli, F., M. Meier, A. Berger, C.L. Rosenberg, and R. Gieré. 2004. U-Th-Pb and  $^{230}\text{Th}/^{238}\text{U}$  Disequilibrium Isotope Systematics: Precise Accessory Mineral Chronology and Melt Evolution Tracing in the Alpine Bergell Intrusion. *Geochim. Cosmochim. Acta* **68**:2543–2560.
- Parsons, T., and Thompson, A. 1993. Does magmatism influence low angle faulting? *Geology* **21**:247–250.
- Paterson, M.S. 2001. A granular flow theory for the deformation of partially melted rock. *Tectonophysics*, **335**:51–61.
- Patino Douce, A.E., and N. Harris. 1998. Experimental constraints on Himalayan anatexis. *J. Petrol.* **39**:689–710.
- Petford, N., A.R. Cruden, K.J.W. McCaffrey, and J.-L. Vigneresse. 2000. Granite magma formation, transport and emplacement in the Earth's crust. *Nature* **408**:669–673.
- Ranalli, G., and D.C. Murphy. 1987. Rheological stratification of the lithosphere. *Tectonophysics* **132**:281–296.

- Renner, J., B. Evans, and G. Hirth. 2000. On the rheologically critical melt fraction. *Earth Planet. Sci. Lett.* **181**:585–594.
- Rey, P., O. Vanderhaeghe, and C. Teyssier. 2001. Gravitational collapse of continental lithosphere: Definition, regimes, and modes. *Tectonophysics* **342**:435–444.
- Riller, U., I. Petrinovic, J. Ramelow, M. Strecker, and O. Oncken. 2001. Late Cenozoic tectonism, collapse caldera and plateau formation in the central Andes. *Earth Planet. Sci. Lett.* **188**:299–311.
- Roscoe, R. 1952. The viscosity of suspensions of rigid spheres. *Brit. J. Appl. Phys.* **3**: 267–269.
- Rosenberg, C.L. 2001. Deformation of partially molten granite: A review and comparison of experimental and natural case studies. *Intl. J. Earth Sci.* **90**:60–76.
- Rosenberg, C.L. 2004. Shear zones and magma ascent: A model based on a review of the Tertiary magmatism in the Alps. *Tectonics* **23**:TC3002, doi10.1029/2003TC001526.
- Rosenberg, C.L., and M.R. Handy. 2005. Experimental deformation of partially melted granite revisited: Implications for the continental crust. *J. Metamorphic Geol.* **23**:19–28. doi:1111/j.1525–1314.2005.005555.x.
- Royden, L. 1996. Coupling and decoupling of crust and mantle in convergent orogens: Implications for strain partitioning in the crust. *J. Geophys. Res.* **101**:17,679–17,705.
- Rushmer, T. 1995. An experimental deformation study of partially molten amphibolite: Application to low-melt fraction segregation. *J. Geophys. Res.* **100**:15,681–15,695.
- Rutter, E. 1997. The influence of deformation on the extraction of crustal melts: A consideration on the role of melt-assisted granular flow. In: *Deformation-enhanced Fluid Transport in the Earth's Crust and Mantle*, ed. M.B. Holness, Mineral. Soc. Ser. 8, pp. 82–110. London: Chapman & Hall.
- Rutter, E., and D.H.K. Neumann. 1995. Experimental deformation of partially molten Westerly granite under fluid-absent conditions, with implications for the extraction of granitic magmas. *J. Geophys. Res.* **100**:15,697–15,715.
- Sawyer, E.W. 2001. Grain-scale and outcrop-scale distribution and movement of melt in a crystallizing granite. *Trans. R. Soc. Edinburgh: Earth Sci.* **91**:73–85.
- Scheuber, E., and P.A.M. Andriessen. 1990. The kinematic and geodynamic significance of the Atacama Fault Zone, northern Chile. *J. Struct. Geol.* **12**:243–257.
- Schilling, F.R., and G.M Partzsch. 2001. Quantifying partial melt fraction in the crust beneath the central Andes and the Tibetan Plateau. *Phys. & Chem. Earth A* **26**: 239–246.
- Schilling, F.R., G.M Partzsch, H. Brasse, and G. Schwarz. 1997. Partial melting below the magmatic arc in the Central Andes deduced from geoelectromagnetic field experiments and laboratory data. *Phys. Earth & Planet. Inter.* **103**:17.
- Schmid, S.M., H.R. Aebli, F. Heller, and A. Zingg. 1989. The role of the Periadriatic Line in the tectonic evolution of the Alps. In: *Alpine Tectonics*, ed. M.P. Coward, D. Dietrich, and R. Park, Spec. Publ. 45, pp. 153–171. London: Geol. Soc.
- Schmid, S.M., and E. Kissling. 2000. The arc of the western Alps in the light of geophysical data on deep crustal structure. *Tectonics* **19**:62–85.
- Schmid, S.M., O.A. Pfiffner, N. Froitzheim, G. Schönborn, and E. Kissling. 1996. Geophysical-geological transect and tectonic evolution of the Swiss-Italian Alps. *Tectonics* **15**:1036–1064.
- Schmitz, M., W.-D. Heinsohn, and F.R. Schilling. 1997. Seismic, gravity, and petrological evidence for partial melt beneath the thickened Central Andean crust (21–23°S). *Tectonophysics* **270**:313–326.

- Scott, T.J., and D.L. Kohlstedt. 2004. The effect of large melt fraction on the deformation behaviour of peridotite: Implications for the viscosity of Io's mantle and the rheologically critical melt fraction. *EOS Trans. AGU* **85**, Fall Meeting suppl., Abstract.
- Searle, M.P., and L. Godin. 2003. The South Tibetan Detachment and the Manaslu Leucogranite: A structural reinterpretation and restoration of the Annapurna-Manaslu Himalaya, Nepal. *J. Geol.* **111**:505–523.
- Solar, G., and M. Brown. 2001. Petrogenesis of migmatites in Maine, USA: Possible source of peraluminous leucogranite in plutons. *J. Petrol.* **42**:789–823.
- Teyssier, C., B. Tikoff, and M. Markley. 1995. Oblique plate motion and continental tectonics. *Geology* **23**:447–450.
- Teyssier, C., and D.L. Whitney. 2002. Gneiss domes and orogeny. *Geology* **30**:1139–1142.
- Tikoff, B., and M. de Saint Blanquat. 1997. Transpressional shearing and strike-slip partitioning in the late Cretaceous Sierra Nevada magmatic arc, California. *Tectonics* **16**:442–459.
- Tirel, C., J.-P. Brun, and E. Burov. 2004. Thermomechanical modeling of extensional gneiss domes. In: *Gneiss Domes in Orogeny*, ed. D. Whitney, C. Teyssier, and S. Siddoway, Spec. Paper 380, pp. 67–78. Boulder, CO: Geol. Soc. Am.
- Tommasi, A., A. Vauchez, L.A.D. Fernandes, and C. Porcher. 1994. Magma-assisted strain localization in an orogen-parallel transcurrent shear zone of southern Brazil. *Tectonics* **13**:421–437.
- Unsworth, M.J., A.G. Jones, W. Wei et al. 2005. Crustal rheology of the Himalaya and Southern Tibet inferred from magnetotelluric data. *Nature* **438**:78–81.
- Vanderhaeghe, O., J.-P. Burg, and C. Teyssier. 1999. Exhumation of migmatites in two collapsed orogens: Canadian Cordillera and French Variscides. In: *Exhumation Processes: Normal Faulting, Ductile Thinning and Erosion*, ed. U. Ring, M.T. Brandon, G.S. Lister, and S.D. Willet, Spec. Publ. 154, pp. 181–204. London: Geol. Soc.
- Vanderhaeghe, O., S. Medvedev, C. Beaumont, P. Fullsack, and R.A. Jamieson. 2003. Evolution of orogenic wedges and continental plateaux: Insights from crustal thermal-mechanical models overlying subducting mantle lithosphere. *Geophys. J. Intl.* **153**:27–51.
- Vanderhaeghe, O., and C. Teyssier. 2001a. Crustal-scale rheological transitions during late-orogenic collapse. *Tectonophysics* **335**:211–228.
- Vanderhaeghe, O., and C. Teyssier. 2001b. Partial melting and flow of orogens. *Tectonophysics* **342**:451–472.
- van der Molen, I., and M.S. Paterson. 1979. Experimental deformation of partially melted granite. *Contrib. Mineral. & Petrol.* **70**:299–318.
- Vauchez, A., S. Pacheco Neves, and A. Tommasi. 1997. Transcurrent shear zones and magma emplacement in Neoproterozoic belts of Brazil. In: *Granite: From Segregation of Melt to Emplacement Fabrics*, ed. J.-L. Bouchez, D.H.W. Hutton, and W.E. Stephens, pp. 275–293. Dordrecht: Kluwer Academic.
- Vigneresse, J.-L., and B. Tikoff. 1999. Strain partitioning during partial melting and crystallization of felsic magmas. *Tectonophysics* **312**:117–132.
- von Blanckenburg, F., H. Kagami, A. Deutsch et al. 1998. The origin of Alpine plutons along the Periadriatic Lineament. *Schweiz. Mineral. Petrograph. Mitt.* **78**:57–68.
- Wernicke, B.P., R.L. Christiansen, P.C. England, and L.J. Sonder. 1987. Tectonomagmatic evolution of Cenozoic extension in the North American Cordillera. In: *Continental Extensional Tectonics*, ed. M.P. Coward, J.F. Dewey, and P.L. Hancock, Spec. Publ. 28, pp. 203–221. London: Geol. Soc.

- White, A.P., and K.V. Hodges. 2002. Multistage extensional evolution of the central East Greenland Caledonides. *Tectonics* **21**:1048, doi:10.1029/2001/C001308.
- Wickham, S.M. 1987. The segregation and emplacement of granitic magmas. *J. Geol. Soc. Lond.* **144**:281–297.
- Willett, S.D., and D.C. Pope. 2004. Thermo-mechanical models of convergent orogenesis: Thermal and rheologic dependence of crustal deformation. In: Rheology and deformation of the lithosphere at continental margins, ed. G.D. Karner, B. Taylor, N.W. Driscoll, and D.L. Kohlstedt, pp. 179–222. New York: Columbia Univ. Press.
- Wu, C., K.D. Nelson, G. Wortman et al. 1998. Yadong cross-structure and South Tibetan Detachment in the east central Himalaya (89–90°E). *Tectonics* **17**:28–45, 97TC03386.
- Yin, A., and M.T. Harrison. 2000. Geologic evolution of the Himalayan-Tibetan orogen. *Ann. Rev. Earth & Planet. Sci.* **28**:211–280.
- Yuan, X., S.V. Sobolev, R. Kind et al. 2000. Subduction and collision processes in the Central Andes constrained by converted seismic phases. *Nature* **408**:958–961.
- Zhang, H., N. Harris, R. Parrish et al. 2004. Causes and consequences of protracted melting of the mid-crust exposed in the North Himalayan antiform. *Earth Planet. Sci. Lett.* **228**:195–212.
- Zimmerman, M.E., and D.L. Kohlstedt. 2004. Rheological properties of partially molten lherzolite. *J. Petrol.* **45**:275–298.